Slowing ageing using drug synergy in *C. elegans*

Tesfahun Dessale[1], Krishna Chaithanya Batchu[2], Diogo Barardo[2], Ng Li Fang[2], Vanessa Yuk Man Lam[2], Markus R. Wenk[1,3,4], Nicholas S. Tolwinski[2,4], Jan Gruber[1,2]

1. Department of Biochemistry, Yong Loo Lin School of Medicine, National University of Singapore, Singapore
2. Science Divisions, Yale-NUS College, Singapore
3. Singapore Lipidomics Incubator, Life Sciences Institute, National University of Singapore, Singapore
4. Department of Biological Sciences, National University of Singapore, Singapore

Summary

Pharmacological interventions that target human ageing should extend individual healthspan and result in dramatic economic benefits to rapidly ageing societies worldwide. For such interventions to be contemplated they need to comprise drugs that are efficacious when given to adults and for which extensive human safety data are available. Here we show that dramatic lifespan extension can be achieved in *C.elegans* by targeting multiple, evolutionarily conserved ageing pathways using drugs that are already in human use. By targeting multiple synergistic ageing pathways, we are able to slow ageing rate, double lifespan and more than double healthspan while avoiding developmental and fitness trade-offs. To the best of our knowledge this is the largest lifespan effect ever reported for any adult-onset drug treatment in *C. elegans*. This drug-repurposing approach, using drugs already approved for humans to target multiple conserved aging pathways simultaneously, could lead to interventions that prevent age-related diseases and overall frailty in a rapidly ageing population.

Key Words: Drug synergy, Transcriptome, ageing, lipidomics

Introduction

Some of ageing research's most important findings are the evolutionarily conserved pathways that regulate lifespan[1-6]. In model organisms, mutations affecting these pathways can often extend lifespan by between 30% and 100%[7,8]. Combining different genetic mutations can result in synergistic lifespan extension[9-11]. By contrast, the effect of pharmacological interventions are typically much weaker, even when targeting the same pathways[2,12,13], but the genetic synergy suggests a potential strategy for the design of novel pharmacological interventions simultaneously targeting multiple evolutionarily conserved ageing pathways. To date there is little data on synergistic effects of pharmacological interventions on lifespan[14]. Here we report an *in vivo* approach to design novel multi-drug ageing interventions. We show how multi-drug interventions leverage pathway synergies to maximize effect size, while minimizing side effects and detrimental developmental tradeoffs by targeting distinct but interacting ageing pathways. Our ultimate aim was to design a purely pharmacological, adult-onset intervention with lifespan efficacy similar or better than those of canonical aging mutations.

Due to the lack of generally accepted biological markers for ageing[15-17], lifespan studies are currently the only way to test the efficacy of ageing interventions[18]. We therefore developed our candidate drug combinations in a short-lived model organism, the nematode *Caenorhabditis elegans*. Using our approach, we identify two triple drug combinations that extend lifespan and healthspan to an extent greater than any previously reported pharmacological intervention in *C. elegans*. Our synergistic drug combinations show effect sizes comparable to the classical ageing mutations while avoiding most of the tradeoffs associated with them[19-21]. We find that these interventions actually increase some markers of performance while slowing biological ageing rate. Moreover, we identified TGFβ as a key contributor and required pathway mediating these synergistic effects. We also showed that worms treated with synergistic drug combinations have higher MUFA:PUFA ratios and a decrease in membrane lipid peroxidation index. Finally, we confirm that this synergistic effect is also present in the fruit fly *Drosophila melanogaster*.

Results

Pathway and compound selection in *C. elegans*

Based on existing literature, we identified a set of well-characterized and evolutionarily conserved ageing pathways and lifespan extension mechanisms (Supplementary Table S1). We chose to target AMP activated protein kinase (AMPK), mammalian target of rapamycin (mTOR), caloric restriction (CR), C-Jun N-terminal kinases (JNK) and mitohormesis/mitochondrial metabolism as primary longevity regulatory pathways. For each pathway, we identified drugs and drug-like molecules reported to extend lifespan in at least one common model organism (nematodes, fruit flies or mice). We were interested in drugs that might eventually be tested in humans so we favored drugs with reported efficacy in mammals or that are already approved for human use. Based on these criteria, we initially selected eleven candidate drugs (Supplementary Table S1). We added allantoin to our study based on a report showing lifespan effects in *C. elegans* and a transcriptional analysis suggesting that its mode of action is distinct from other compounds[22]. In order to test the lifespan effects, as these can be highly sensitive to details in experimental conditions and can be variable between different laboratories[19,23], we first carried out operator-blinded confirmatory lifespan studies using the previously reported optimal dose. We found that only five compounds extended lifespan reproducibly under conditions used in our laboratory (Fig. 1, Extended data Fig. 1, Supplementary Table S2). Generally, lifespan extension effects in our hands tended to be smaller compared to previous reports[7,22,24-26] (Fig. 1, Extended data Fig. 1, Supplementary Table S2).

Transcriptome, Drug synergy and longevity

To examine drug modes of action, we carried out transcriptomics analysis and determined differentially expressed genes (DEG) and pathway enrichments relative to untreated controls. Rifampicin (RIF) and rapamycin (RAP) followed by psora-4 (PSORA) caused the most extensive changes in gene expression, both at the gene and pathway level, while metformin (MET) and allantoin (ALLAN) showed comparatively smaller effects on gene expression (Fig. 2a Supplementary Table S3). While transcriptional analyses revealed significant overlap between affected genes, we also identified sets of genes that were unique to each individual compound (Fig. 2a). MET shows significant overlap with the other drugs, having the smallest unique set. Almost all genes affected by MET and PSORA were also affected by at least one other drug in the set (Fig. 2a). ALLAN causes fewer gene-expression changes than any of the other compounds, but most of these changes are unique, with fewer than half of the genes also affected by any of the other compounds (Fig. 2a). Effects of RIF and RAP were quite different from each other and from any of the other drugs. We confirmed this by principle component analysis (PCA) which showed that RIF, RAP and PSORA are well separated by the first three principle components. ALLAN and MET, by contrast, are more variable and very close to each other and to untreated control (Fig. 2b, Extended data Fig. 4c).

We next determine effect of different drug combinations on life span in nematodes. We began with MET and RAP due to their translational importance in humans[14,27]. However, RAP combined with MET at their optimal doses did not show further benefit on lifespan (Extended data Fig. 2j,p). We carried out additional trials, exploring all possible combinations of optimal and half-optimal dose for MET and RAP (Extended data Fig. 2j-p). Combination of RAP and MET each at their half-optimal dose result in further extension in maximum lifespan (Fig. 2e, Extended data Fig. 2m,s) but did not result in further mean lifespan extension (Extended data 2p). These weak benefits of combining MET with RAP are consistent with results in mice where the existing evidence suggests that addition of MET to RAP results in some additional benefits mainly in males with only weak (if any) additional benefits in females[14].

We then systematically determined the efficacy of all ten possible pairs out of the five candidate drugs (Extended data Fig. 2a-i). We define synergy based on the Higher Single Activity (HSA) model[28];

Drug combinations are considered synergistic if the combinatorial effect is significantly larger than any of the combination's single drug effect at the same (ideal) concentrations as in the combination. Using this definition, we identified two synergistic combinations out of the ten pairs tested (Fig. 2c, d, Extended data Fig. 2 and Supplementary Table S2). The synergistic pairs comprise RIF and either RAP or PSORA. This means that two out of the three pairs formed by the drugs that are most well-separated in the PCA are synergistic (Fig. 2b, Extended data Fig. 4a,b). Of the remaining eight combinations, four extended lifespan as much as their best component while the other four combinations nullified each other and did not result in lifespan extension and none were toxic (Extended data Fig. 2, Supplementary Table S2).

Lifespan extension resulting from the two synergistic pairs, while larger than those of previously published drug effects, were still smaller than the benefits seen with genetic mutations[9]. This raises the question whether this represented the maximum achievable by adult-onset drug treatment or if further benefits could be gained by adding additional compounds. Since exhaustive combinatorial search of all thirty possible triple drug combinations was not feasible, we explored selected triple combinations based in the original synergistic pairs. We first evaluated the combination of the three drugs best separated by PCA and involved in the two initial synergistic pairs (RAP, RIF and PSORA). However, nematodes treated with this triple combination had a shorter lifespan than seen with either of the dual combinations (Extended data Fig. 3a Supplementary Table S2). We then tested three drug combinations including ALLAN as the unique gene set of ALLAN (light orange arc in Fig. 2a) shows no overlap at the level of GO terms (blue links) with the other drugs or with *eat-2,* suggesting ALLAN has a unique mode of action[22]. We tested addition of ALLAN to the two double compound, synergistic combinations. This addition resulted in significant additional mean and maximum lifespan extension in both cases (Figures 2f,g, Extended data Fig. 3d-f and Supplementary Table S2). The best triple combination (RAP, RIF, ALLAN) doubles mean lifespan, resulting in a median lifespan of up to 44 days and a maximum lifespan of 50 days (Supplementary Table S2). This is comparable to the canonical ageing mutations and is, to the best of our knowledge, the largest lifespan extension ever reported in *C. elegans* with any adult-onset drug intervention[29].

Mechanisms of drug synergy

Daf-16/FOXO is a transcription factor that plays a key role in lifespan determination in model organisms and likely also in humans[30,31]. To explore the mode of action of our synergistic drug combinations we determined their dependence on *daf-16* in mutant worms deficient in this pathway. Individually, RAP and ALLAN lifespan extension was *daf-16*-independent while RIF lifespan extension was fully and PSORA was partially *daf-16* dependent (Fig. 3a, Extended data Fig. 8). The synergistic combination RAP+RIF comprising one *daf-16* dependent (RIF) and one *daf-16* independent drug (RAP), and even the RIF+PSORA combination of two *daf-16* dependent drugs, still showed synergistic lifespan extension in *daf-16* mutants (Fig. 3a, Extended data Fig. 8). This surprising data suggest that synergies can be *daf-16* independent, even if individual constituent drugs are *daf-16* dependent.

Several of the drugs tested have previously been reported to be CR mimetics[17,32-34]. We therefore tested each synergistic combination and its constituent compounds in a *C. elegans* model of CR (*eat-2* mutants). We found that only RIF among the single drug treatments further extended lifespan in *eat-2* mutants (Fig 3b, Extended data Fig. 8), suggesting that all except RIF may function as CR mimetic. The synergistic combinations both comprise one CR mimetic with one non-CR mimetic (RAP+RIF and RIF+PSORA). Only RIF+PSORA resulted in further lifespan extension and addition of ALLAN, a second CR mimetic, did not result in further benefits.

To further explore the mechanism of drug synergy we determine the transcriptome profile for each synergistic and selected non-synergistic drug combination. Transcriptomic analysis in worms treated with single, double and triple drug exposure for the synergistic and non-synergistic combinations

revealed that the transcriptome of CR mimetic single drugs is clustered together with *eat-2*, whereas the non-CR mimetic RIF is different from *eat-2* and from all other single drugs (Fig. 2h). Interestingly, the transcriptome of synergistic combinations are clustered together and the pattern is different from those of their constituent single drugs and from that of *eat-2* mutants (Fig. 2h, Extended data Fig. 4c,d). Moreover, we found that only the TFGβ pathway was commonly enriched in synergistic dual and triple combinations (Fig. 4a, Extended data Fig. 6c, 7a, Supplementary Table S4) relative to control. To identify pathways that were further enriched by the drug combinations relative to their constituent single drugs, we used the single drug transcriptome as background control (see methods) for pathway analysis. Using this approach, we found that synergistic combinations affected TGFβ and additional pathways relative to their parent drugs while none of the non-synergistic combinations did so (Supplementary Table S5). Because some drug combinations resulted in further lifespan extension in *eat-2* mutants relative to their constituent drugs, we tested whether TGFβ was enriched in the transcriptomes of N2 animals treated with synergistic drug combinations relative to untreated *eat-2* worms. Again, TGFβ was the only pathway enriched in all synergistic combinations (Extended data Fig. 7b Supplementary Table S6). Overall, we found that the TGFβ signaling pathway was commonly and exclusively enriched in synergistic combinations (Fig. 4b, Extended data Fig. 7a,c, Supplementary Table S7).

TGFβ is required for drug synergy

The specific and consistent enrichment of TGFβ suggests that TGFβ may play a role in mediating the observed synergistic lifespan extension. Previously it has been shown that TGFβ (*daf-7*) mutation extends lifespan *via* insulin signaling and that both *daf-2* and *daf-7* regulate the transcription of *daf-16* dependent genes[35] (Extended data Fig. 7d). To test the role of the IGF pathway in this effect and to determine if the lifespan of already long-lived *daf-2* mutants could be further extended using our drug combinations, we first determined lifespan of *daf-2* mutants for each combination. Only the RAP-based combinations, RAP+RIF and RAP+RIF+ALLAN, showed lifespan extension in *daf-2* mutants. However, the effect size was similar to that of RAP alone and none of the combinations resulted in further synergy (Fig. 3c, Extended data Fig. 8, Supplementary Table S2). PSORA treatment alone extended the lifespan of *daf-2* mutants, but none of the PSORA based combinations, RIF+PSORA and RIF+PSORA+ALLAN, extended lifespan in *daf-2* mutants (Fig. 3c and Extended data Fig. 8). We next tested the efficacy of all synergistic combinations and their components in *daf-7* mutants. None of the combinations show synergistic effects in the *daf-7* mutants, suggesting that synergy requires *daf-7,* even if drugs singularly still extend lifespan (Fig. 3d, Extended data Fig. 8).

Drug synergy, MUFA and health span

Long-lived mutants such as *age-1* and *daf-2* have previously been shown to exhibit metabolic perturbations resulting in increased production and storage of fats[36]. Furthermore, TGFβ/*daf-7* regulates triacylglycerol (TAG) metabolism[37] and *daf-7* mutants are known to store more fats[36]. These links in conjunction with our transcriptomics data led us to investigate whether treatment with synergistic drug combinations resulted in modifications in lipid profiles consistent with TGFβ inhibition. (Supplementary Table S3). First we explored the transcriptomics data for changes that might affect lipid composition and found that synergistic drug combinations resulted in a significant up regulation of the *C. elegans* SREBP-1c homolog - *sbp-1*, a master transcription factor controlling several lipogenic genes, and genes coding for "desaturases" responsible for MUFA synthesis[38-40] (Fig. 4c,e). We then employed an MS-based lipidomics assay to determine changes in lipid compositions resulting from drug treatments. Worm that were exposed to the synergistic drug combinations have a significant rise in TAG reserves (Fig. 4d), a marked increase in the MUFA:PUFA ratios (Fig 4g) and a significant increase in 16:1 and 19:1 -MUFAs (Fig. 4f). Because of these changes there was a

significant decline in the calculated double bond index (DBI) as well as the lipid peroxidation index (PI) (Fig. 4i). A low PI, indicates that lipids contain fewer carbon-carbon double bonds, making them less susceptible to peroxidation and this has been previously associated with increased life span, probably related to lower susceptibility to lipid peroxidation[41,42,43]. A reduction in the susceptibility to lipid peroxidation suggests better resistance to oxidative stress[44,45] and worms treated with synergistic drug combinations indeed showed such an increase in resistance (Fig. 5f). We also observed an increase in total sphingomyelin (Fig. 4h); an event that has previously shown to elicit autophagy-dependent lifespan extension in the nematodes[46].

Suppression of energy metabolism and inhibition of the electron transport chain (ETC) can extend lifespan in *C. elegans*[47,48]. In our experiments, however, drug treatments did not have significant effects on basal metabolic rate (Fig. 5i), excluding this explanation. The most common tradeoffs related with lifespan extension are developmental delay, slower growth rate and reduced fecundity[49,50,51]. We found that worms treated with either of the synergistic drug combinations did not show any significant effect on adult size or total fertility although combination treatments slightly extended reproductive span (Fig. 5a-c, Extended data Fig. 9a).

Next, we assessed several parameters of fitness, stress resistance and health: speed of spontaneous movement, tolerance to heat shock and oxidative stress resistance and a motility based health span score based on the scoring scheme of Herndon *et al*[52]. Control animals spent about 50% of their lifespan in the optimal (best) health category while nematodes exposed to the RIF+PSORA+ALLAN and RAP+RIF+ALLAN spent 57% and 63%, respectively, of their already extended lifespan in optimal health (Fig. 5d, Extended data 9c). This means that their healthspan was significantly extended both in absolute and relative terms. Indeed, more than half of the treated animals were still in optimal health even after the last control animal had died (Fig. 5d, Extended data Fig. 9c). Animals treated with RAP+RIF+ALLAN and RIF+PSORA+ALLAN also performed significantly better in the spontaneous movement assay than control animals at most ages. In fact, old treated animals (day 18 of age) showed performance in this assay that was indistinguishable from young (day 7) controls (Fig. 5g). Moreover, treated animals experienced improvements in resistance to heat and oxidative stress (paraquat assay, Figure 5e,f, Extended data Fig. 9b). These observations indicate that animals treated with synergistic drug combinations not only enjoyed greater lifespan with limited or no detected tradeoffs, but also improved health span, increased stress resistance, and even increased physical performance. Such observations raise the important question if lifespan effect are due to an actual delay in biological ageing rate. The rate of ageing can be expressed as mortality rate doubling time (MRDT). We determined MRDT of animals exposed to synergistic drug combinations using Survcurv[53], and found MRDT to be significantly longer in RIF+PSORA+ALLAN treated animals compared to controls (MRDT of control = 3 days and RIF+PSORA+ALLAN = 3.7 days, P value < 0.0001). We found that the initial mortality rate was also significantly lower ((IMR of control = $2.7e^{-3}$, IMR of RIF+PSORA+ALLAN = $8.5e^{-4}$, RAP+RIF+ALLAN = $9.3e^{-4}$, P value < 0.001). This means that synergistic drug combinations extend lifespan by making worms age more slowly while also making them more robust when young (Extended data Fig. 10).

Drug synergy is conserved in Drosophila

One of the key questions for ageing studies is whether lifespan effects are conserved across species. We therefore tested whether the synergistic lifespan extensions we found in *C. elegans* are conserved in *Drosophila melanogaster*. RAP has previously been shown to extend lifespan of fruit flies[54] while MET has been shown to be ineffective[55]. We systematically tested all single drugs and all synergistic combinations in male fruit flies. First, we showed that RAP and ALLAN extend mean lifespan whereas RIF and PSORA extend only the maximum lifespan of flies (Fig. 6 Supplementary Table S2). However, the RAP based combinations RAP+RIF and RAP+RIF+ALLAN showed conserved

synergistic lifespan extension in flies (Fig. 6a). The PSORA based combinations; RIF+PSORA and RIF+PSORA+ALLAN did not show further mean lifespan extension (Fig. 6b). However, RIF+PSORA showed synergistic maximum lifespan extension compared to single drugs (Fig. 6c). This data confirms that our strategy was able to identify evolutionary conserved synergies.

Discussion

By targeting multiple overlapping ageing and longevity-related pathways we succeeded in designing synergistic pharmacological interventions that, even when only applied to animals from adult age, more than doubled healthy lifespan in *C. elegans*. This effect size is comparable to that of the classical ageing mutations and, to the best of our knowledge, is the largest reported for any adult-onset pharmacological intervention[13]. However, unlike in ageing mutatiants we were not able to detect any detrimental evolutionary or fitness tradeoffs associated with lifespan extensions by drug synergies [19]. The benefits are also not due to ETC or other metabolic suppression as judged by oxygen consumption rate[47,48]. In fact, treated animals outperform age-matched controls in some performance assays and old treated animals have the physical appearance and performance comparable to much younger controls (Fig. 5g). Mortality analysis suggests that synergistic drug treatments slow basic biological ageing rate by ~20% (Extended data Fig. 10). To test for evolutionary conservation, we determined lifespan benefits in the fruit fly *Drosophila melanogaster*, confirming qualitative conservation for two of the four synergistic drug combinations. Nematodes are evolutionarily more distant from fruit flies than they are from mammals[56], making mechanisms and pathways conserved between flies and nematodes ancient, and tracing this synergy back to a common ancestor of all three clades.

To explore the mechanism of these synergistic lifespan benefits, we carried out epistasis experiments and transcriptomic analysis, finding that *daf-2*/*daf-16* (IGF/FOXO) as well as the TGFβ pathway (*daf-7*) are involved in synergistic lifespan extension (Fig. 4j). The connection between IGF/FOXO and TGFβ is consistent with previous results where *daf-7* regulates lifespan *via* insulin signaling[35], neuronal TGFβ links food availability and longevity[57], and *daf-7* regulates metabolism in *C. elegans* and controls fat accumulation[36]. Several previous studies have demonstrated that lifespan extending mutations in *C. elegans* result in alterations in lipid metabolism causing an increase in the MUFA and reduction in PUFA levels[58,59]. In agreement with this, drug synergies resulted in an up regulation of *sbp-1*, a master transcription factor controlling several genes related to lipid metabolism and MUFA synthesis[38-40] (Fig. 4c,e, Extended data Fig. 5). MS-based lipidomics analysis of nematodes exposed to synergistic drug combinations revealed major changes consistent with activation of *sbp-1,* including accumulation of TAGs and increases in the MUFA:PUFA ratios (both in PC and PE classes). In humans, high ratios of MUFA:PUFA have also been found in erythrocyte membranes of children of nonagenarians[60,61].

There has been much interest in the potential for MET and possibly RAP to delay age-dependent decline and disease in humans. Given this translational interest, the limited benefit of combining MET with RAP in both *C. elegans* and mice is somewhat disappointing.

However, as our results illustrate, lifespan is determined through complex and interactive biochemical and gene regulatory networks. Intervening simultaneously at multiple points of these networks can result in significant and sometimes surprising benefits[28,62]. Our proof-of-principle study suggests that beneficial synergistic and additive interactions affecting key longevity pathways are unexpectedly common and evolutionarily conserved. These data support the feasibility of targeting multiple conserved ageing pathways using existing drugs to slow down biological ageing rate, an approach that, if translatable to humans, would result in dramatic medical and economic benefits[63].

Tables and figures

Figure 1: Single drugs extend lifespan of wild type *C. elegans*

Wild type N2 worms treated with different doses of **a**, RAP **b**, RIF **c**, MET **d**, PSORA and **e**, ALLAN have longer lifespan. **f**, Mean lifespan of worms treated with the optimal dose of each drug, mean ± SD. Each drug treatments resulted in a statistically significant lifespan extension at their optimal dose. **P < 0.001, ***P < 0.0001, log-rank.

Figure 2: Double and triple drug combinations showed synergistic lifespan extension; a, Circos plot illustrating gene overlap for single drugs and *eat-2* mutant transcriptome. Purple lines link genes shared by multiple drugs. Blue lines link different genes which fall into the same GO term. A greater number of purple and blue links and longer dark orange arcs indicates greater overlap among the DGE and GO terms of each drug. (Minimum overlap = 3, minimum enrichment = 1.5, P value < 0.01). **b**, Three dimensional principle component analysis based on DGE (PCA). **c**, RAP+RIF and **d**, RIF+PSORA results in synergistic lifespan extension (P<0.0001, log-rank). **e**, RAP+MET did not show further mean lifespan extension but showed further maximum lifespan extension compared to single drug treatments. **f**, RIF+PSORA+ALLAN and **g**. RAP+RIF+ALLAN showed synergistic lifespan extension (P<0.0001, log-rank). **h**, Heatmap showing hierarchical clustering (distance metrics and linkage algorithms) of single drugs and synergistic combinations. n = 2000 for RNASeq and 50-100 for lifespan studies. *P<0.01, **P<0.001, ***P<0.0001

Figure 3: Drug combinations did not show synergy on *daf-7*, *daf-2* and *daf-16* mutants. a, all dual and triple synergistic combinations resulted in lifespan extension in *daf-16* mutants but effect size does not exceed individual drug effects. **b**, Of the single drugs only RIF extends lifespan of *eat-2* (P<0.05, log-rank). RIF+PSORA resulted in synergistic lifespan extension in *eat-2* mutants (P<0.05, log-rank). **c**, None of the synergistic combinations showed synergy in *daf-2* mutants. **d**, RIF alone extends lifespan of *daf-7* mutants (P<0.05, log-rank) but combinations fail to result in further synergistic lifespan extension. At least 50 worms per condition.

Figure 4: Transcriptomics and lipidomics profiles explain the mechanism of drug synergy. a, Venn diagram for pathways enriched by synergistic drug combinations. Only TGFβ is commonly enriched in all synergistic combinations. **b**, Heatmap of pathways enriched by synergistic drug combinations compared to their constituent single drugs. Only TGFβ is commonly enriched in all synergistic combinations. **c**, Mechanism of MUFA containing lipid accumulation and lifespan extension. **d**, Total triacylglycerol content normalized to the control, three biological replicates, 2500 worms per condition, (Mean ± SD, one-way ANOVA) **e**, Fat metabolism-related gene expression profile, log fold change, P value < 0.05. **f**, Fatty acid species abundance normalized to control, three biological replicates, 2500 worms per condition (Mean ± SD, one-way ANOVA). **g**, Phosphatidylcholine species abundance based on double bond, three biological replicates, 2500 worms per condition (Mean ± SD, one-way ANOVA). **h**, Total sphingomyelin content normalized to the control, three biological replicates, 2500 worms per condition, (Mean ± SD, one-way ANOVA). **i**, Double bond index, per oxidation index and MUFA/PUFA ratios calculated for phosphatidylcholine species for all conditions, MUFA/PUFA is normalized to the control. Three biological replicates,

2500 worms per condition (Mean ± SD), **j**. Hypothesized mechanism of lifespan extension by drug synergies. Red–inhibition, green–activation, black–unknown. *P<0.01, **P<0.001, ***P<0.0001.

Figure 5: RIF+PSORA+ALLAN and RAP+RIF+ALLAN improve healthspan without tradeoffs. a-c, RIF+PSORA+ALLAN and RAP+RIF+ALLAN shows extension of reproductive span but no effect on total fertility, n=10 worms per condition. **d**, health span, n>150 worms per condition, P<0.0001, one-way ANOVA. **e**, resistance to heat stress, n=50 worms per condition. **f**, resistance to paraquat stress, n=50 worms per condition. **g**, distance travelled n=50 worms per condition, one-way ANOVA. **h**, development measured by size of worms n=10 worms per condition. **i**, basal metabolic rate, n=80 worms per condition, one-way ANOVA. *P<0.01, **P<0.001, ***P<0.0001

Figure 6: Drug synergies resulted in conserved lifespan extension in *Drosophila melanogaster*. a,b,c RAP extends both mean and maximum lifespan. RAP+RIF and RAP+RIF+ALLAN resulted in synergistic mean and maximum lifespan extension. RIF and PSORA did not extend mean lifespan of flies. Their combination also did not extend mean lifespan. However, RIF and PSORA extends maximum lifespan significantly. RIF+PSORA and RIF+PSORA+ALLAN resulted in further maximum lifespan extension, close to additive (P value < 0.001) but not mean lifespan. n = 80 flies per condition. *P<0.01, **P<0.001, ***P<0.0001

Reference

1 Bitto, A., Wang, A. M., Bennett, C. F. & Kaeberlein, M. Biochemical Genetic Pathways that Modulate Aging in Multiple Species. *Cold Spring Harbor perspectives in medicine* **5**, doi:10.1101/cshperspect.a025114 (2015).

2 DiLoreto, R. & Murphy, C. T. The cell biology of aging. *Molecular biology of the cell* **26**, 4524-4531, doi:10.1091/mbc.E14-06-1084 (2015).

3 Kennedy, B. K. & Lamming, D. W. The Mechanistic Target of Rapamycin: The Grand ConducTOR of Metabolism and Aging. *Cell metabolism* **23**, 990-1003, doi:10.1016/j.cmet.2016.05.009 (2016).

4 Greer, E. L. & Brunet, A. Signaling networks in aging. *Journal of cell science* **121**, 407-412, doi:10.1242/jcs.021519 (2008).

5 Partridge, L. & Gems, D. Mechanisms of ageing: public or private? *Nature reviews. Genetics* **3**, 165-175, doi:10.1038/nrg753 (2002).

6 Guarente, L. & Kenyon, C. Genetic pathways that regulate ageing in model organisms. *Nature* **408**, 255-262, doi:10.1038/35041700 (2000).

7 Robida-Stubbs, S. *et al.* TOR signaling and rapamycin influence longevity by regulating SKN-1/Nrf and DAF-16/FoxO. *Cell metabolism* **15**, 713-724, doi:10.1016/j.cmet.2012.04.007 (2012).

8 Dorman, J. B., Albinder, B., Shroyer, T. & Kenyon, C. The age-1 and daf-2 genes function in a common pathway to control the lifespan of Caenorhabditis elegans. *Genetics* **141**, 1399-1406 (1995).

9 Hou, L. *et al.* A Systems Approach to Reverse Engineer Lifespan Extension by Dietary Restriction. *Cell metabolism* **23**, 529-540, doi:10.1016/j.cmet.2016.02.002 (2016).

10 Sagi, D. & Kim, S. K. An engineering approach to extending lifespan in C. elegans. *PLoS genetics* **8**, e1002780, doi:10.1371/journal.pgen.1002780 (2012).

11 Chen, D. *et al.* Germline signaling mediates the synergistically prolonged longevity produced by double mutations in daf-2 and rsks-1 in C. elegans. *Cell reports* **5**, 1600-1610, doi:10.1016/j.celrep.2013.11.018 (2013).

12 Tacutu, R. *et al.* Human Ageing Genomic Resources: integrated databases and tools for the biology and genetics of ageing. *Nucleic acids research* **41**, D1027-1033, doi:10.1093/nar/gks1155 (2013).
13 Barardo, D. *et al.* The DrugAge database of aging-related drugs. *Aging cell* **16**, 594-597, doi:10.1111/acel.12585 (2017).
14 Strong, R. *et al.* Longer lifespan in male mice treated with a weakly estrogenic agonist, an antioxidant, an alpha-glucosidase inhibitor or a Nrf2-inducer. *Aging cell* **15**, 872-884, doi:10.1111/acel.12496 (2016).
15 Burkle, A. *et al.* MARK-AGE biomarkers of ageing. *Mechanisms of ageing and development* **151**, 2-12, doi:10.1016/j.mad.2015.03.006 (2015).
16 Lopez-Otin, C., Blasco, M. A., Partridge, L., Serrano, M. & Kroemer, G. The hallmarks of aging. *Cell* **153**, 1194-1217, doi:10.1016/j.cell.2013.05.039 (2013).
17 Longo, V. D. *et al.* Interventions to Slow Aging in Humans: Are We Ready? *Aging cell* **14**, 497-510, doi:10.1111/acel.12338 (2015).
18 Hansen, M. & Kennedy, B. K. Does Longer Lifespan Mean Longer Healthspan? *Trends in cell biology* **26**, 565-568, doi:10.1016/j.tcb.2016.05.002 (2016).
19 Gruber, J., Ng, L. F., Poovathingal, S. K. & Halliwell, B. Deceptively simple but simply deceptive--Caenorhabditis elegans lifespan studies: considerations for aging and antioxidant effects. *FEBS letters* **583**, 3377-3387, doi:10.1016/j.febslet.2009.09.051 (2009).
20 Mukhopadhyay, A. & Tissenbaum, H. A. Reproduction and longevity: secrets revealed by C. elegans. *Trends in cell biology* **17**, 65-71, doi:10.1016/j.tcb.2006.12.004 (2007).
21 Walker, D. W., McColl, G., Jenkins, N. L., Harris, J. & Lithgow, G. J. Evolution of lifespan in C. elegans. *Nature* **405**, 296-297, doi:10.1038/35012693 (2000).
22 Calvert, S. *et al.* A network pharmacology approach reveals new candidate caloric restriction mimetics in C. elegans. *Aging cell* **15**, 256-266, doi:10.1111/acel.12432 (2016).
23 Gruber, J. *et al.* Caenorhabditis elegans: What We Can and Cannot Learn from Aging Worms. *Antioxidants & redox signaling* **23**, 256-279, doi:10.1089/ars.2014.6210 (2015).
24 Golegaonkar, S. *et al.* Rifampicin reduces advanced glycation end products and activates DAF-16 to increase lifespan in Caenorhabditis elegans. *Aging cell* **14**, 463-473, doi:10.1111/acel.12327 (2015).
25 Onken, B. & Driscoll, M. Metformin induces a dietary restriction-like state and the oxidative stress response to extend C. elegans Healthspan via AMPK, LKB1, and SKN-1. *PloS one* **5**, e8758, doi:10.1371/journal.pone.0008758 (2010).
26 Ye, X., Linton, J. M., Schork, N. J., Buck, L. B. & Petrascheck, M. A pharmacological network for lifespan extension in Caenorhabditis elegans. *Aging cell* **13**, 206-215, doi:10.1111/acel.12163 (2014).
27 Barzilai, N., Crandall, J. P., Kritchevsky, S. B. & Espeland, M. A. Metformin as a Tool to Target Aging. *Cell metabolism* **23**, 1060-1065, doi:10.1016/j.cmet.2016.05.011 (2016).
28 Alexis A. Borisy, P. J. E., Nicole W. Hurst, Margaret S. Lee, Joseph Leha´r, E. Roydon Price, George Serbedzija, & Grant R. Zimmermann, M. A. F., Brent R. Stockwell, and Curtis T. Keith. Systematic discovery of multicomponent therapeutics. *PNAS* **100**, 7977–7982, doi:10.1073/pnas.1337088100 (June 24, 2003).
29 Barardo, D. *et al.* The DrugAge database of aging-related drugs. *Aging cell*, doi:10.1111/acel.12585 (2017).
30 Martins, R., Lithgow, G. J. & Link, W. Long live FOXO: unraveling the role of FOXO proteins in aging and longevity. *Aging cell* **15**, 196-207, doi:10.1111/acel.12427 (2016).
31 Brunet, A. [Aging and the control of the insulin-FOXO signaling pathway]. *Medecine sciences : M/S* **28**, 316-320, doi:10.1051/medsci/2012283021 (2012).
32 Fontana, L. & Partridge, L. Promoting health and longevity through diet: from model organisms to humans. *Cell* **161**, 106-118, doi:10.1016/j.cell.2015.02.020 (2015).

33 Madeo, F., Pietrocola, F., Eisenberg, T. & Kroemer, G. Caloric restriction mimetics: towards a molecular definition. *Nature reviews. Drug discovery* **13**, 727-740, doi:10.1038/nrd4391 (2014).
34 Ingram, D. K. & Roth, G. S. Calorie restriction mimetics: can you have your cake and eat it, too? *Ageing research reviews* **20**, 46-62, doi:10.1016/j.arr.2014.11.005 (2015).
35 Shaw, W. M., Luo, S., Landis, J., Ashraf, J. & Murphy, C. T. The C. elegans TGF-beta Dauer pathway regulates longevity via insulin signaling. *Current biology : CB* **17**, 1635-1645, doi:10.1016/j.cub.2007.08.058 (2007).
36 Kimura, K. D., Tissenbaum, H. A., Liu, Y. & Ruvkun, G. daf-2, an insulin receptor-like gene that regulates longevity and diapause in Caenorhabditis elegans. *Science (New York, N.Y.)* **277**, 942-946 (1997).
37 Ishikawa, T., Mizunoya, W., Shibakusa, T., Inoue, K. & Fushiki, T. Transforming growth factor-beta in the brain regulates fat metabolism during endurance exercise. *American journal of physiology. Endocrinology and metabolism* **291**, E1151-1159, doi:10.1152/ajpendo.00039.2006 (2006).
38 Ashrafi, K. *et al.* Genome-wide RNAi analysis of Caenorhabditis elegans fat regulatory genes. *Nature* **421**, 268-272, doi:10.1038/nature01279 (2003).
39 Nomura, T., Horikawa, M., Shimamura, S., Hashimoto, T. & Sakamoto, K. Fat accumulation in Caenorhabditis elegans is mediated by SREBP homolog SBP-1. *Genes & nutrition* **5**, 17-27, doi:10.1007/s12263-009-0157-y (2010).
40 McKay, R. M., McKay, J. P., Avery, L. & Graff, J. M. C elegans: a model for exploring the genetics of fat storage. *Developmental cell* **4**, 131-142 (2003).
41 Zimniak, P. Detoxification reactions: relevance to aging. *Ageing research reviews* **7**, 281-300, doi:10.1016/j.arr.2008.04.001 (2008).
42 Jove, M. *et al.* Plasma long-chain free fatty acids predict mammalian longevity. *Scientific reports* **3**, 3346, doi:10.1038/srep03346 (2013).
43 Halliwell, B. & Gutteridge, J. *Free Radicals in Biology and Medicine*. 5th edn, (Oxford University Press, 2015).
44 Hulbert, A. J., Pamplona, R., Buffenstein, R. & Buttemer, W. A. Life and death: metabolic rate, membrane composition, and life span of animals. *Physiological reviews* **87**, 1175-1213, doi:10.1152/physrev.00047.2006 (2007).
45 Pamplona, R., Barja, G. & Portero-Otin, M. Membrane fatty acid unsaturation, protection against oxidative stress, and maximum life span: a homeoviscous-longevity adaptation? *Annals of the New York Academy of Sciences* **959**, 475-490 (2002).
46 Mosbech, M. B. *et al.* Functional loss of two ceramide synthases elicits autophagy-dependent lifespan extension in C. elegans. *PloS one* **8**, e70087, doi:10.1371/journal.pone.0070087 (2013).
47 Lee, S. J., Hwang, A. B. & Kenyon, C. Inhibition of respiration extends C. elegans life span via reactive oxygen species that increase HIF-1 activity. *Current biology : CB* **20**, 2131-2136, doi:10.1016/j.cub.2010.10.057 (2010).
48 Rea, S. L., Ventura, N. & Johnson, T. E. Relationship between mitochondrial electron transport chain dysfunction, development, and life extension in Caenorhabditis elegans. *PLoS biology* **5**, e259, doi:10.1371/journal.pbio.0050259 (2007).
49 Lee, Y. *et al.* Inverse correlation between longevity and developmental rate among wild C. elegans strains. *Aging* **8**, 986-999, doi:10.18632/aging.100960 (2016).
50 Ball, Z. B., Barnes, R. H. & Visscher, M. B. The effects of dietary caloric restriction on maturity and senescence, with particular reference to fertility and longevity. *The American journal of physiology* **150**, 511-519 (1947).
51 Thondamal, M., Witting, M., Schmitt-Kopplin, P. & Aguilaniu, H. Steroid hormone signalling links reproduction to lifespan in dietary-restricted Caenorhabditis elegans. *Nature communications* **5**, 4879, doi:10.1038/ncomms5879 (2014).

52 Herndon, L. A. *et al.* Stochastic and genetic factors influence tissue-specific decline in ageing C. elegans. *Nature* **419**, 808-814, doi:10.1038/nature01135 (2002).
53 Ziehm, M. & Thornton, J. M. Unlocking the potential of survival data for model organisms through a new database and online analysis platform: SurvCurv. *Aging cell* **12**, 910-916, doi:10.1111/acel.12121 (2013).
54 Bjedov, I. *et al.* Mechanisms of life span extension by rapamycin in the fruit fly Drosophila melanogaster. *Cell metabolism* **11**, 35-46, doi:10.1016/j.cmet.2009.11.010 (2010).
55 Slack, C., Foley, A. & Partridge, L. Activation of AMPK by the putative dietary restriction mimetic metformin is insufficient to extend lifespan in Drosophila. *PloS one* **7**, e47699, doi:10.1371/journal.pone.0047699 (2012).
56 Wang, D. Y., Kumar, S. & Hedges, S. B. Divergence time estimates for the early history of animal phyla and the origin of plants, animals and fungi. *Proceedings. Biological sciences* **266**, 163-171, doi:10.1098/rspb.1999.0617 (1999).
57 Entchev, E. V. *et al.* A gene-expression-based neural code for food abundance that modulates lifespan. *eLife* **4**, e06259, doi:10.7554/eLife.06259 (2015).
58 Shmookler Reis, R. J. *et al.* Modulation of lipid biosynthesis contributes to stress resistance and longevity of C. elegans mutants. *Aging* **3**, 125-147, doi:10.18632/aging.100275 (2011).
59 Hillyard, S. L. & German, J. B. Quantitative lipid analysis and life span of the fat-3 mutant of Caenorhabditis elegans. *Journal of agricultural and food chemistry* **57**, 3389-3396, doi:10.1021/jf8031414 (2009).
60 Gonzalez-Covarrubias, V. Lipidomics in longevity and healthy aging. *Biogerontology* **14**, 663-672, doi:10.1007/s10522-013-9450-7 (2013).
61 Puca, A. A. *et al.* Fatty acid profile of erythrocyte membranes as possible biomarker of longevity. *Rejuvenation research* **11**, 63-72, doi:10.1089/rej.2007.0566 (2008).
62 Bansal, M. *et al.* A community computational challenge to predict the activity of pairs of compounds. *Nat Biotechnol* **32**, 1213-1222, doi:10.1038/nbt.3052 (2014).
63 Goldman, D. P. *et al.* Substantial health and economic returns from delayed aging may warrant a new focus for medical research. *Health affairs (Project Hope)* **32**, 1698-1705, doi:10.1377/hlthaff.2013.0052 (2013).

Supplementary Information

Supplementary Methods

Culturing *C. elegans*

For all experiments Bristol N2 wild-type or mutant nematodes were grown and maintained on Nematode Growth Medium (NGM) agar plates at 20°C using *E. coli* OP50 bacteria as food source unless otherwise noted. After plates were poured and dried, they were sealed and stored at 4°C. *E. coli* were spotted on plates on the previous evening and allowed to dry. For compound treatments, all agar plates were prepared from the same batch of NGM agar and treatment plates were supplemented with the respective compounds or vehicle as a control. Fresh plates were prepared every week. The following worm strains were used: wild type N2, *eat-2* (DA1116), *daf-2* (CB1370), *daf-16* (CF1038), *daf-7* (CB1372). The strain CB1372 was provided by Takao Inoue. All the other strains were obtained from the Caenorhabditis Genetics Center (CGC).

Bacterial Preparation Method

A single colony OP50 *E. coli* was picked and incubated at 37°C for 20 hours with shaking at 180 rpm in LB broth supplemented with Streptomycin (final concentration 200μg/ml). Bacterial colony forming units (CFU) were determined spectrophotometrically at 600nm wavelength, and bacterial stock was diluted to 10^{10}, and frozen at -80°C. NGM plates were seeded with bacteria and used for lifespan assays without further incubation. Drugs or vehicles were added to the bacteria (in addition to being added to NGM) just before seeding.

Determination of lifespan

For determination of *C. elegans* lifespan, nematodes were age synchronized by bleaching, allowed to hatch and 150-200 young adult worms per condition were transferred to 3-5 35mm culture plates. Worms were transferred to fresh plates every day until progeny production ceased, and every two to three days afterwards, until all worms had died. The number of worms that were alive was determined every day, and dead worms were removed from the plate. Worms were considered dead when no touch-provoked movement was observed. Animals that crawled off the plate, exhibited extruded internal organs or displayed an egg laying defective with subsequent hatching of larvae inside the mother were censored. All lifespan assays were blinded and repeated at least two times. Graph pad Prism 5.0 software was used to calculate mean adult lifespan and to perform statistical analysis of significance using the log-rank test (Mantel-Cox).

Compound identification and validation

Primary Screening: First, we identified well-characterized ageing regulatory pathways (Extended data Table-1). Next, we identified drugs and drug-like molecules that are known to target the selected pathways and to extend lifespan in a common ageing model organisms (worm, fly or mice). Some compounds that had been reported to target known ageing

pathways and had not yet been experimentally validated as lifespan-extending were also included. This approached culminated in the identification of 11 candidate drugs (Extended data Table-1). Primary efficacy was confirmed in terms of lifespan in *C. elegans*. Initial screening of compounds for their effect on lifespan of wild type N2 nematodes were conducted using standardized condition in the presence of antibiotics (200mg/ml streptomycin). Of these 11 drugs and drug-like molecules, only five resulted in reproducible lifespan extension in our lab (Fig. 1). For those compounds that passed the primary screening, dose-response assays were carried out to establish the ideal dose and maximum effect size.

Resistance to oxidative stress

Age-synchronized adult worms were transferred to a fresh NGM plate containing drug or vehicle. 5-fluoro-2'-deoxyuridine (Fudr) was also added to prevent egg hatching. After 48 hours of treatment, worms were transferred to plates with 20mM paraquat (methyl viologen dichloride hydrate, Sigma Aldrich) to induce oxidative stress in the worms. Thereafter, dead worms were counted every day until all of the worms were dead.

Heat shock stress resistance

Age-synchronized adult worms were picked from a NGM plate and transferred to a fresh NGM plate containing drug or vehicle. After 48 hours of treatment, worms were transferred to 37°C incubator for 2 hours to induce heat stress. After heat shock worms were transferred back to 20°C. Survival rates were determined after 24 hours, 48 hours and 72 hours of recovery and compared between the control and drug-treated worm groups.

Fertility assay

Age-synchronized day 3 worms were picked from NGM plate and transferred to fresh NGM plate containing drug or vehicle. A single worm was used per plate with 10 plates per condition. Worms were transferred to a fresh NGM plate containing drug or vehicle every day until they ceased egg laying. Eggs produced by each single worm were incubated at 20°C for 48 hours, and the number of live progeny produced was recorded on each day.

Development by size

Age-synchronized L2 worms were transferred to fresh NGM plates containing drug or vehicle. We took images of worms every day, starting from day 4, the first day of drug treatment for all experiments, up to day 11. Length of worms was determined using the free curve tool provided by the Leica Application Suite software (Leica Microsystems). We compared the mean size of worms under different treatments with the size of untreated control worms in each day using t-test.

Respiration rate

Worms were treated with drug or vehicle for 24 hours. We transfer worms to 96 well assay plates, nine worms per plate at least eight wells per condition. Respiration rates were determined using Seahorse XF96 respirometer following standard protocol[1].

Synergy statistical analysis

To determine whether a drug combination is synergistic first we determined the percent lifespan extension by each individual drug and compared this effect to the effect of their

combination. We consider a combination of drugs to be synergistic if the lifespan effect under combinational treatment is significantly greater than the lifespan effect of the more efficacious of the individual drugs. For triple drug combinations, we test the combined effects against the sum of the effects of the best pair out of the three drugs.

Mortality

We experimentally determined the mortality rate of one of our most powerful interventions, RIF+PSORA+ALLAN, using a large cohort of over 1,000 worms per condition. Dead worms were counted every day until all worms were dead. For RAP+RIF+ALLAN the combined lifespan data was imported to Survecurv for mortality analysis and maximum lifespan comparison[2, 3]. We used the Gompertz survival model to determine the initial mortality rate and mortality rate doubling time using the following equation.

$M(t) = ae^{bt}$
MRD = ln2/b, where
a = baseline hazard rate
b = rate if exponential increase in mortality
t = time
M(t) = mortality rate
MRD = mortality rate doubling time

RNA Extraction and RNAseq

Freshly prepared bacteria (OP50 *E. coli*) were spotted on 94 cm NGM agar plates on the previous evening and allowed to dry. Synchronized, young adult worms were transferred to fresh plates. For maintaining synchronized populations, Fluorodeoxyuridine (FudR) was added to NGM media. After two days of treatment with drug or vehicle adult worms were washed off the plates to 15□ml tubes and washed several times until a clear solution, that indicates bacteria is completely removed, was obtained. Clean worm pellets were then frozen and used for RNA extraction. Total RNA was isolated using Qiagen RNAeasy micro kit (Qiagen, Hilden, Germany) following the standard protocol. Afterwards, RNA was quantified photometrically with NanoDrop 2000 and stored at -80°C until use. The integrity of total RNA was measured by Agilent Bioanalyzer 2100. For library preparation an amount of 2μg of total RNA per sample was processed using Illumina's RNA Sample Prep Kit following the manufacturer's instruction (Illumina, San Diego, CA, USA). All single drugs were processed together and multiplexed onto one lane to minimize batch effect. The different drug combinations were processed into two multiplexed lanes. In total, we ran three lanes in parallel with 20 samples in each and we had untreated N2 controls in each lane. Libraries were sequenced using Illumina HiSeq4000 sequencing platform (Illumina, San Diego, CA, USA) in a paired end read approach at a read length of 150 nucleotides. Sequence data was extracted in FastQ format. The RNA-Seq reads from each sample were mapped to the reference *C. elegans* transcriptome (WBcel235) with *kallisto* (v0.43.0)[4] using 100 bootstrap samples and sequence based bias correction. The estimated counts were imported from kallisto to the R environment (v3.3.2) and summarized to gene-level using the *tximport* package (v1.2.0)[5]. The *DESeq2* package (v1.14.1)[6] was used to identify differentially expressed genes (DEGs) in all our analysis (correcting for batch effects, when applicable) for a significance threshold α of 0.05 after correcting for multiple hypothesis testing through

Independent Hypothesis Weighting (IHW package v1.2.0)[7]. The PCA plot were graphed by the *pcaExplorer* package (v2.0.0) on DESeq2 'rlog' transformed data.

Analysis with known lifespan-extending genes

All 569 *Caenorhabditis elegans* genes that extend lifespan when intervened upon were downloaded from GenAge (build 18)[5] and of those, 512 were verified to be present in our genes expression datasets, and this subset of genes were used exclusively in order to graph the respective heatmap. The heatmaps only used gene expression counts (after DESeq2 normalization and replacement of outliers) for this subset of genes. All the samples of each condition were aggregated by taking the medium values of gene expression counts.

Pathway Analysis

KEGG pathways and GO terms enriched by each drug and drug combination were determined by DAVID [8] and Metascape [9]. To determine pathways enriched in combinations compared to single drugs, we used the differentially expressed genes by single drugs as a background control. To determine the pathways enriched by the synergistic drug combinations compared to *eat-2* we used the genes differentially expressed in untreated *eat-2* vs untreated N2 worms as a background. Venn diagram of pathways done online using (http://bioinformatics.psb.ugent.be/webtools/Venn/)

Lipid extraction and Mass spectrometry

Lipid extraction – young adult day 4 worms, 2,500 per condition, were treated with drug or vehicle for 48 hours. Nematodes were collected, washed with M9 buffer and transferred to 2-mL polypropylene tubes containing 250μl lysis buffer (20mM Tris-HCl pH 7.4, 100mM NaCl, 0.5mM EDTA, 5% glycerol) and left on ice for 15 minutes followed by homogenization using a Bead beater maintained at 4°C. Lipids extraction from the lysed samples was carried out by Folch's extraction[10]. In order to minimize oxidation during and after extraction, 0.5% butylated hydroxytoluene was added to the organic solvents. The upper phase was removed, and to the lower phase a theoretical upper phase was added, vortexed and centrifuged at 3000rpm for 5 minutes. The lower phase was then transferred to a tube, evaporated and dried under vacuum to avoid lipid oxidation. For quantification purposes, the organic phase was spiked with a labeled internal standard corresponding to each lipid class during the single phase extraction so as to control lipid-class dependent differences in extraction and ionization[11]. Standards used were PC-34:0, PE-28:0, SM-30:1, Cer-35:1, DAG-24:0 and TAG-51:0. Subsequently, the samples were evaporated under a speed-valco (Thermo Savant, Milford, USA) and reconstituted in 50μl methanol and left at -80°C until further analysis.

Data acquisition – An Agilent 1260-Ultra Performance Liquid chromatography (UPLC) coupled to Triple Quad Mass spectrometer (Agilent 6490) with dynamic multiple reaction monitoring (dMRM) was used for lipid quantification. The UPLC system was equipped with a Waters ACQUITY BEH C18column (1.0 × 100 mm) to separate the molecular species using gradient elution. Solvent A was acetonitrile/H2O (60:40) with 10mM ammonium formate and 1% NH_4OH, while solvent B was isopropanol/acetonitrile (90:10) containing 10mM ammonium formate and 1% NH_4OH. The flow rate was 0.13mL/min and the column temperature 60°C. Solvent B was set at 40% at injection and increased linearly to 100% in 14

minutes, retained at this value for 3 minutes, decreased back to 40% in one minute and then retained there till the end of the gradient by 20 minutes. The eluent was directed to the ESI source of the mass spectrometer operated in the positive ion mode. The MS conditions were as follows. For ESI: gas temperature, 300°C; gas flow, 10 l/minutes; sheath gas temperature, 350°C; sheath gas flow, 8 l/minutes; and capillary voltage, 3,500 V. For APCI: gas temperature, 300°C; vaporizer, 450°C; gas flow, 5 l/minutes; capillary voltage, 4,000 V; and corona current, 4 μA. Data processing, including peak smoothing and integration of areas under the curves for each ion measured, was performed using the MassHunter Quantification Software (Agilent).

Table-3 Reagents and Resources

Drugs and Compounds	**Source**	**Identifier**
Aspirin	Sigma	A2093
Loxapine Succinate	Sigma	27833-64-3
Psora-4	ApexBio	B7659
Metformin	Sigma	D150959
Rapamycin	LC Laboratories	R-5000
Rifampicin	Sigma	R3501
Allantoin	Fluka	05670
Torin 1	APExBIO	A8312
Mainserin	Sigma	M2525
cAMP	Sigma	A9501
Juglone	Sigma	H47003
Paraquate	Sigma	75365-73-0
Commercial assays		
RNeasy micro kit	QIAGEN	74004
QuantiTect Rev. Transcription Kit	QIAGEN	205311
Agilent RNA 6000 Nano Kit	Agilent Technology	5067-1511
Experimental Models: Organisms/Strains		
C. elegans: Bristol wild-type	CGC	N2
C. elegans: *daf-2*(*e1370*)III	CGC	CB1370
C. elegans: *daf-16*(*mu86*) I	CGC	CF1038
C. elegans: *daf-7*(*e1372*) III	CGC	CB1372
C. elegans: *eat-2* (*ad1116*) II	CGC	DA1116
D. melanogaster:	Male	Oregon-R
Software and Algorithms		
GraphPad Prism 5	GraphPad Software	https://www.graphpad.com/scientificsoftware/prism/
Excel 2016	Microsoft	https://products.office.com/en-us/excel

Supplementary References

1. Koopman, M., et al., *A screening-based platform for the assessment of cellular respiration in Caenorhabditis elegans.* Nat Protoc, 2016. **11**(10): p. 1798-816.
2. Ziehm, M., et al., *SurvCurv database and online survival analysis platform update.* Bioinformatics, 2015. **31**(23): p. 3878-80.
3. Ziehm, M. and J.M. Thornton, *Unlocking the potential of survival data for model organisms through a new database and online analysis platform: SurvCurv.* Aging Cell, 2013. **12**(5): p. 910-6.
4. Bray, N.L., et al., *Near-optimal probabilistic RNA-seq quantification.* Nat Biotechnol, 2016. **34**(5): p. 525-7.
5. Soneson, C., M.I. Love, and M.D. Robinson, *Differential analyses for RNA-seq: transcript-level estimates improve gene-level inferences.* F1000Res, 2015. **4**: p. 1521.
6. Love, M.I., W. Huber, and S. Anders, *Moderated estimation of fold change and dispersion for RNA-seq data with DESeq2.* Genome Biol, 2014. **15**(12): p. 550.
7. Ignatiadis, N., et al., *Data-driven hypothesis weighting increases detection power in genome-scale multiple testing.* Nat Methods, 2016. **13**(7): p. 577-80.
8. Huang da, W., B.T. Sherman, and R.A. Lempicki, *Systematic and integrative analysis of large gene lists using DAVID bioinformatics resources.* Nat Protoc, 2009. **4**(1): p. 44-57.
9. Tripathi, S., et al., *Meta- and Orthogonal Integration of Influenza "OMICs" Data Defines a Role for UBR4 in Virus Budding.* Cell Host Microbe, 2015. **18**(6): p. 723-35.
10. Folch, J., M. Lees, and G.H. Sloane Stanley, *A simple method for the isolation and purification of total lipides from animal tissues.* J Biol Chem, 1957. **226**(1): p. 497-509.
11. Ejsing, C.S., et al., *Collision-induced dissociation pathways of yeast sphingolipids and their molecular profiling in total lipid extracts: a study by quadrupole TOF and linear ion trap-orbitrap mass spectrometry.* J Mass Spectrom, 2006. **41**(3): p. 372-89.

Figure 1

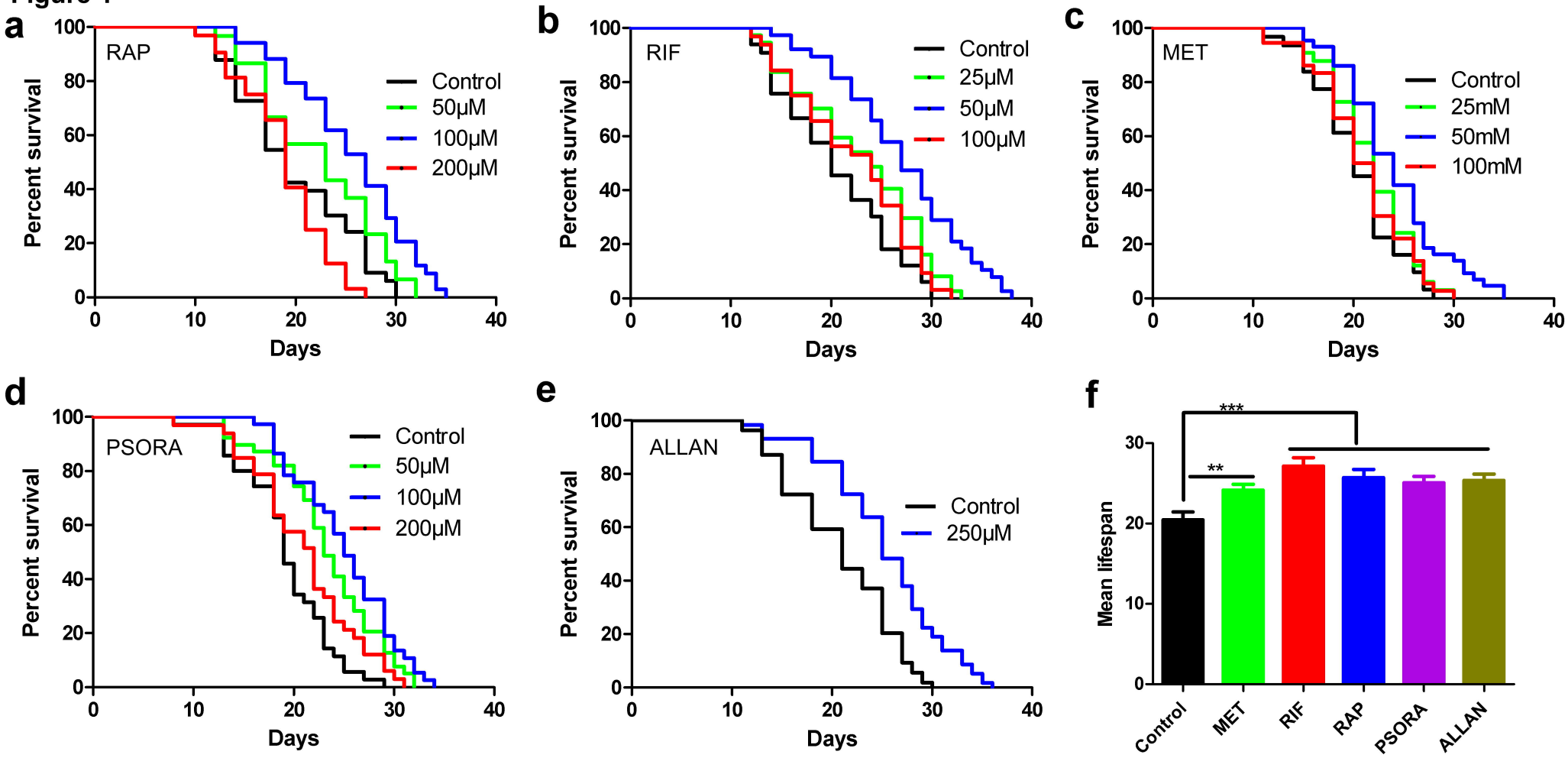
a
RAP
Control
50μM
100μM
200μM
Percent survival
Days
b
RIF
Control
25μM
50μM
100μM
Percent survival
Days
c
MET
Control
25mM
50mM
100mM
Percent survival
Days
d
PSORA
Control
50μM
100μM
200μM
Percent survival
Days
e
ALLAN
Control
250μM
Percent survival
Days
f
Mean lifespan
***
**
Control
MET
RIF
RAP
PSORA
ALLAN

Figure 2

a

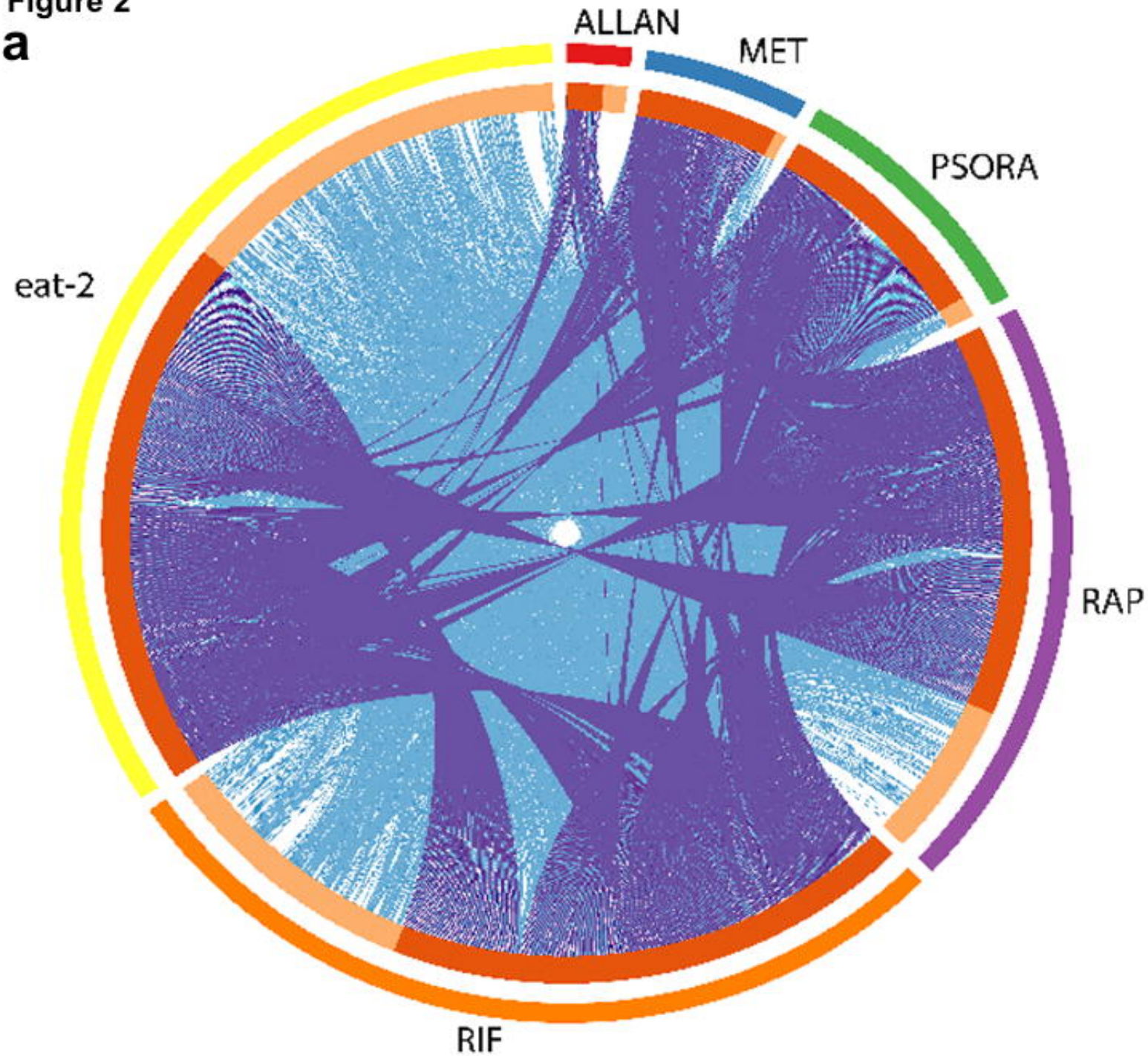

Figure 2

b

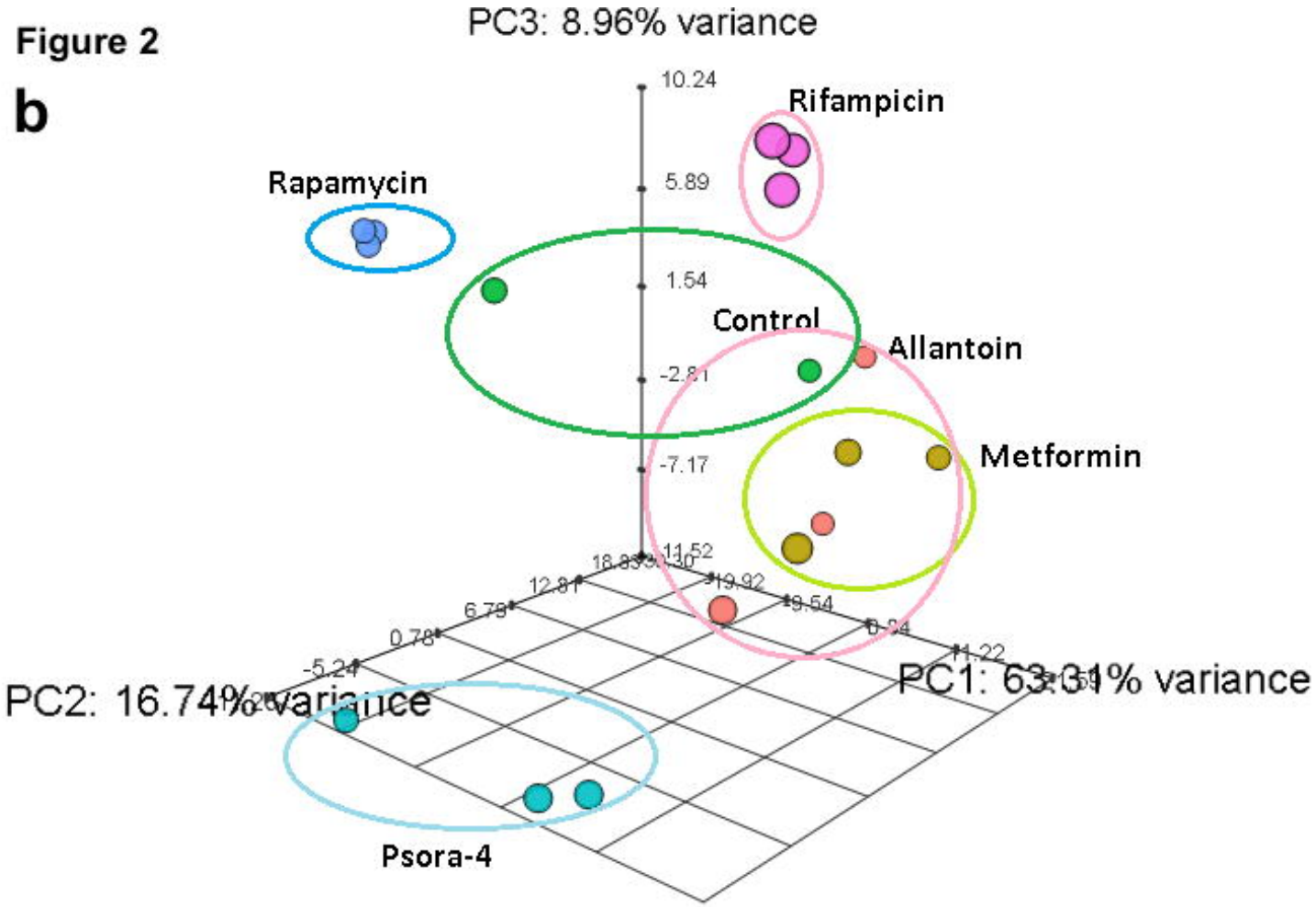
PC3: 8.96% variance
10.24
5.89
1.54
-2.81
-7.17
-11.52
Rifampicin
Rapamycin
Control
Allantoin
Metformin
Psora-4
PC2: 16.74% variance
PC1: 63.31% variance
-5.24
0.78
6.78
12.81
18.83
19.92
19.54
11.22

Figure 2

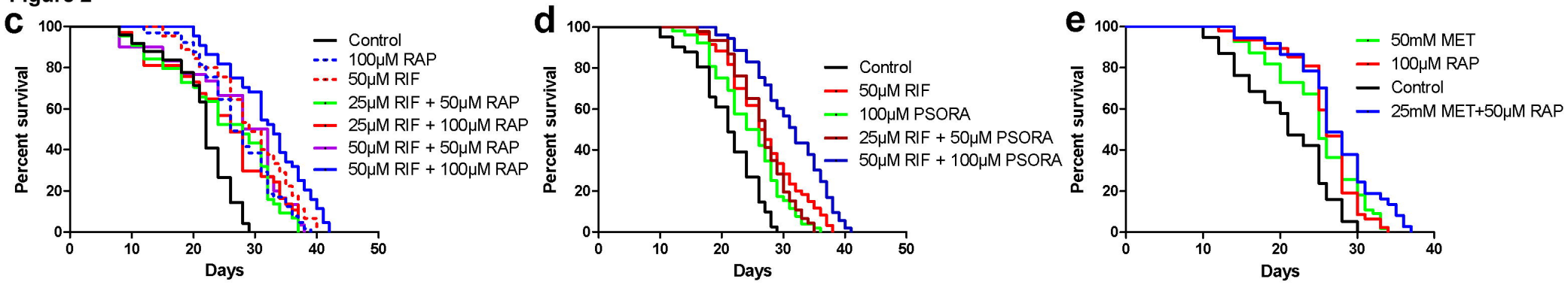
c
Percent survival
Days
Control
100μM RAP
50μM RIF
25μM RIF + 50μM RAP
25μM RIF + 100μM RAP
50μM RIF + 50μM RAP
50μM RIF + 100μM RAP
d
Percent survival
Days
Control
50μM RIF
100μM PSORA
25μM RIF + 50μM PSORA
50μM RIF + 100μM PSORA
e
Percent survival
Days
50mM MET
100μM RAP
Control
25mM MET+50μM RAP

Figure 2

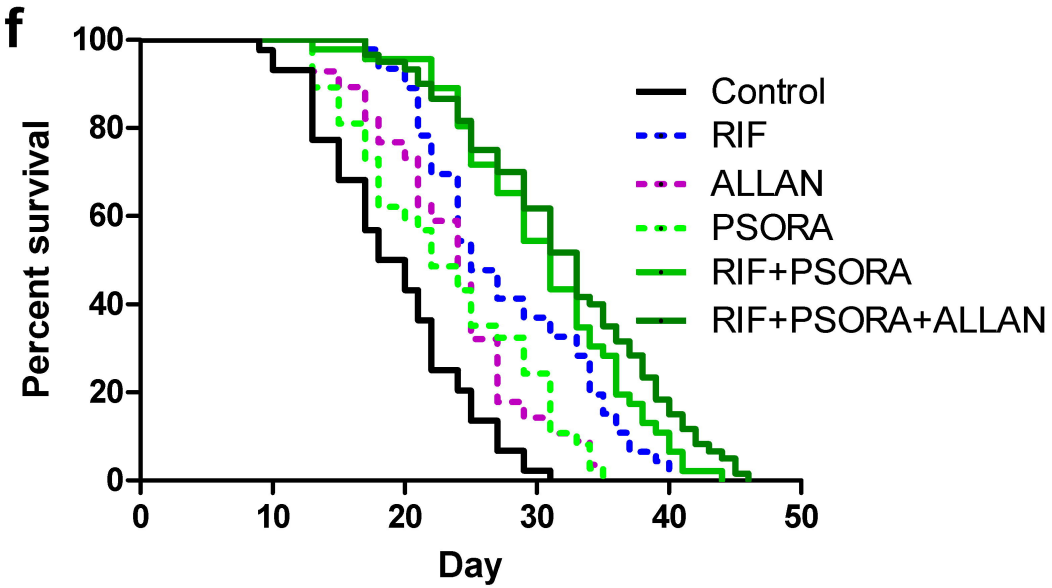
f
Percent survival
100
80
60
40
20
0
0
10
20
30
40
50
Day
Control
RIF
ALLAN
PSORA
RIF+PSORA
RIF+PSORA+ALLAN

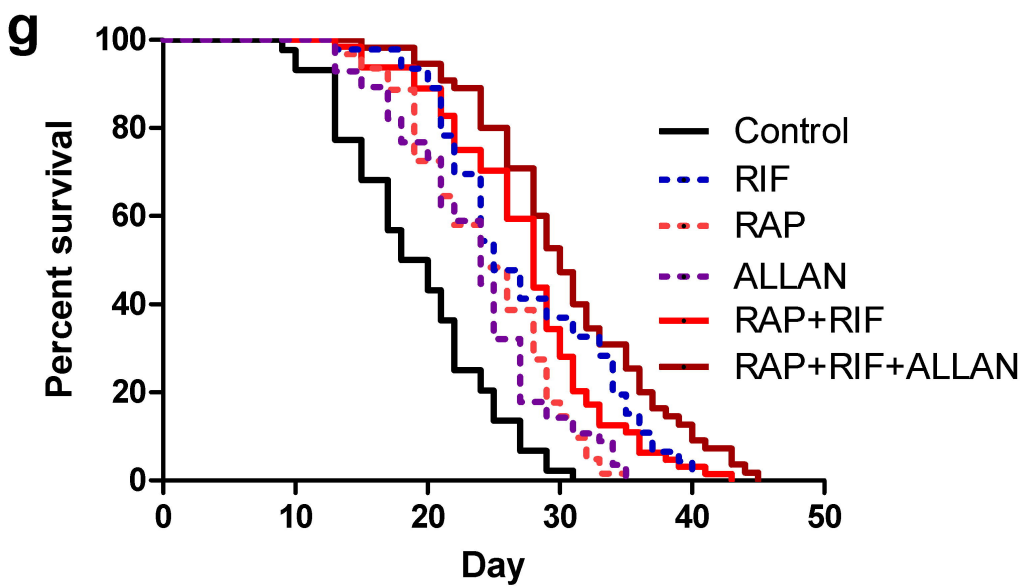
g
Percent survival
100
80
60
40
20
0
0
10
20
30
40
50
Day
Control
RIF
RAP
ALLAN
RAP+RIF
RAP+RIF+ALLAN

Figure 2

h

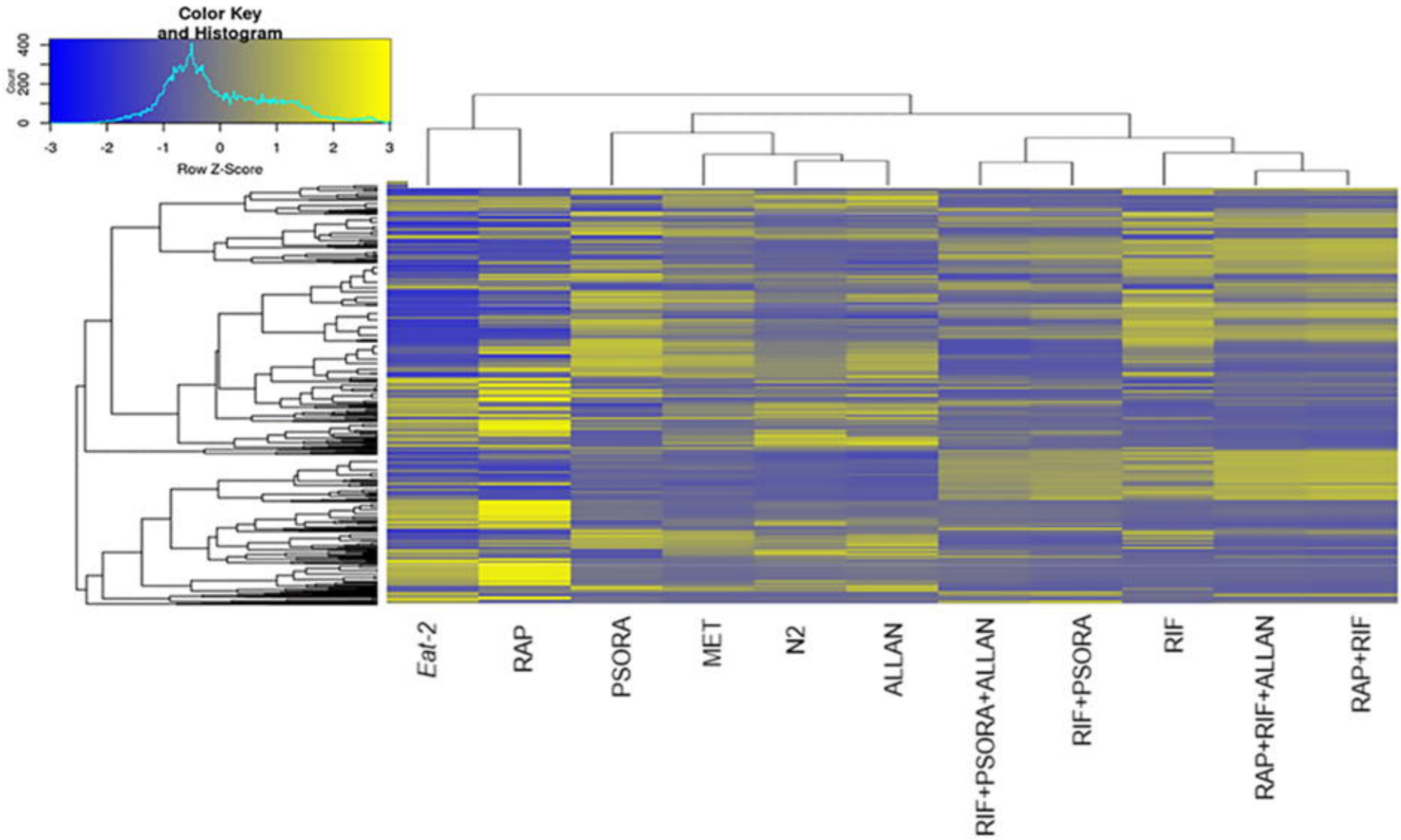
Color Key
and Histogram
Count
400
200
0
-3
-2
-1
0
1
2
3
Row Z-Score
Eat-2
RAP
PSORA
MET
N2
ALLAN
RIF+PSORA+ALLAN
RIF+PSORA
RIF
RAP+RIF+ALLAN
RAP+RIF

Figure 3

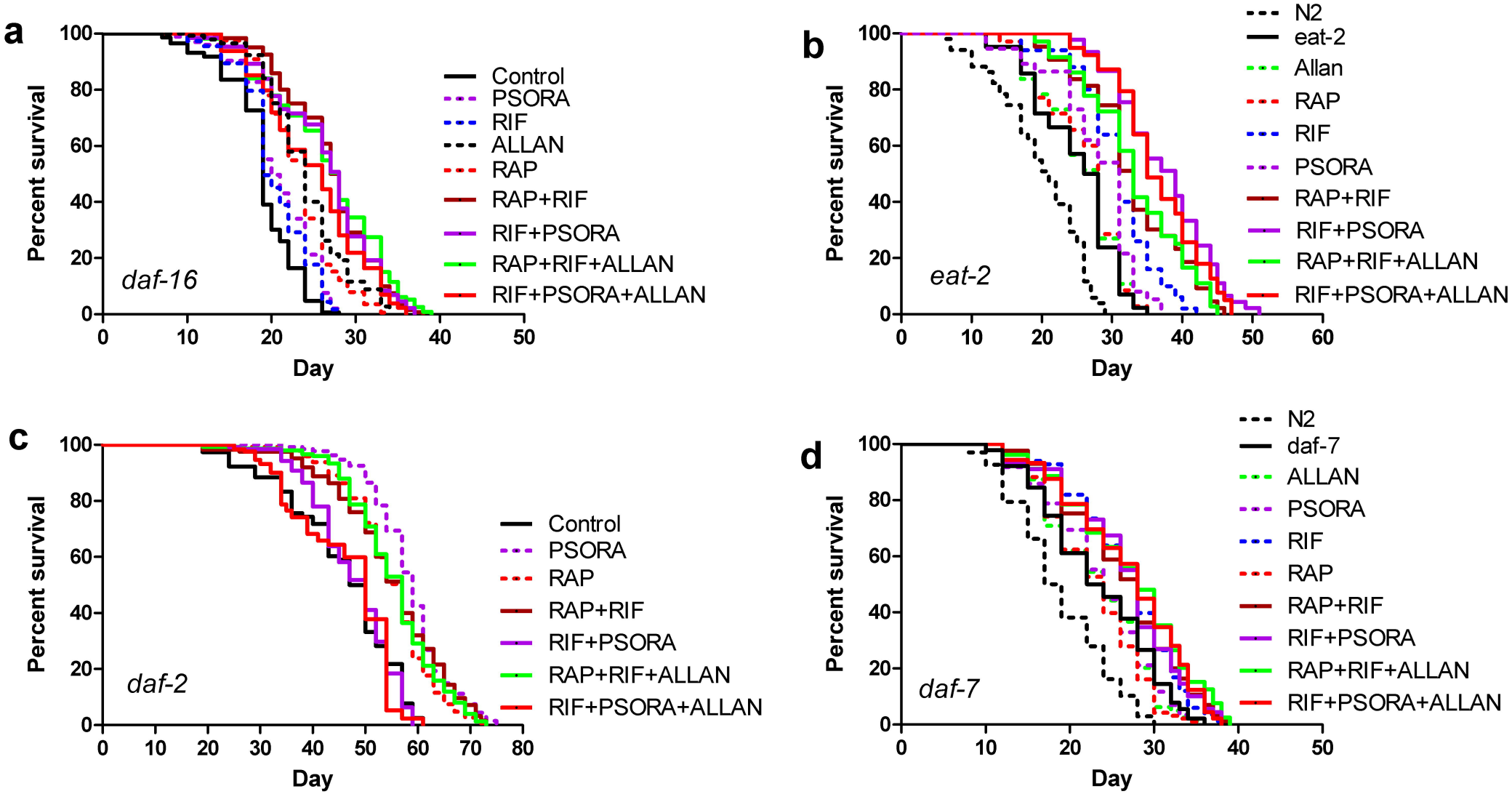
a
Percent survival
Day
daf-16
Control
PSORA
RIF
ALLAN
RAP
RAP+RIF
RIF+PSORA
RAP+RIF+ALLAN
RIF+PSORA+ALLAN
b
eat-2
N2
eat-2
Allan
RAP
RIF
PSORA
RAP+RIF
RIF+PSORA
RAP+RIF+ALLAN
RIF+PSORA+ALLAN
c
daf-2
Control
PSORA
RAP
RAP+RIF
RIF+PSORA
RAP+RIF+ALLAN
RIF+PSORA+ALLAN
d
daf-7
N2
daf-7
ALLAN
PSORA
RIF
RAP
RAP+RIF
RIF+PSORA
RAP+RIF+ALLAN
RIF+PSORA+ALLAN

Figure 4

a

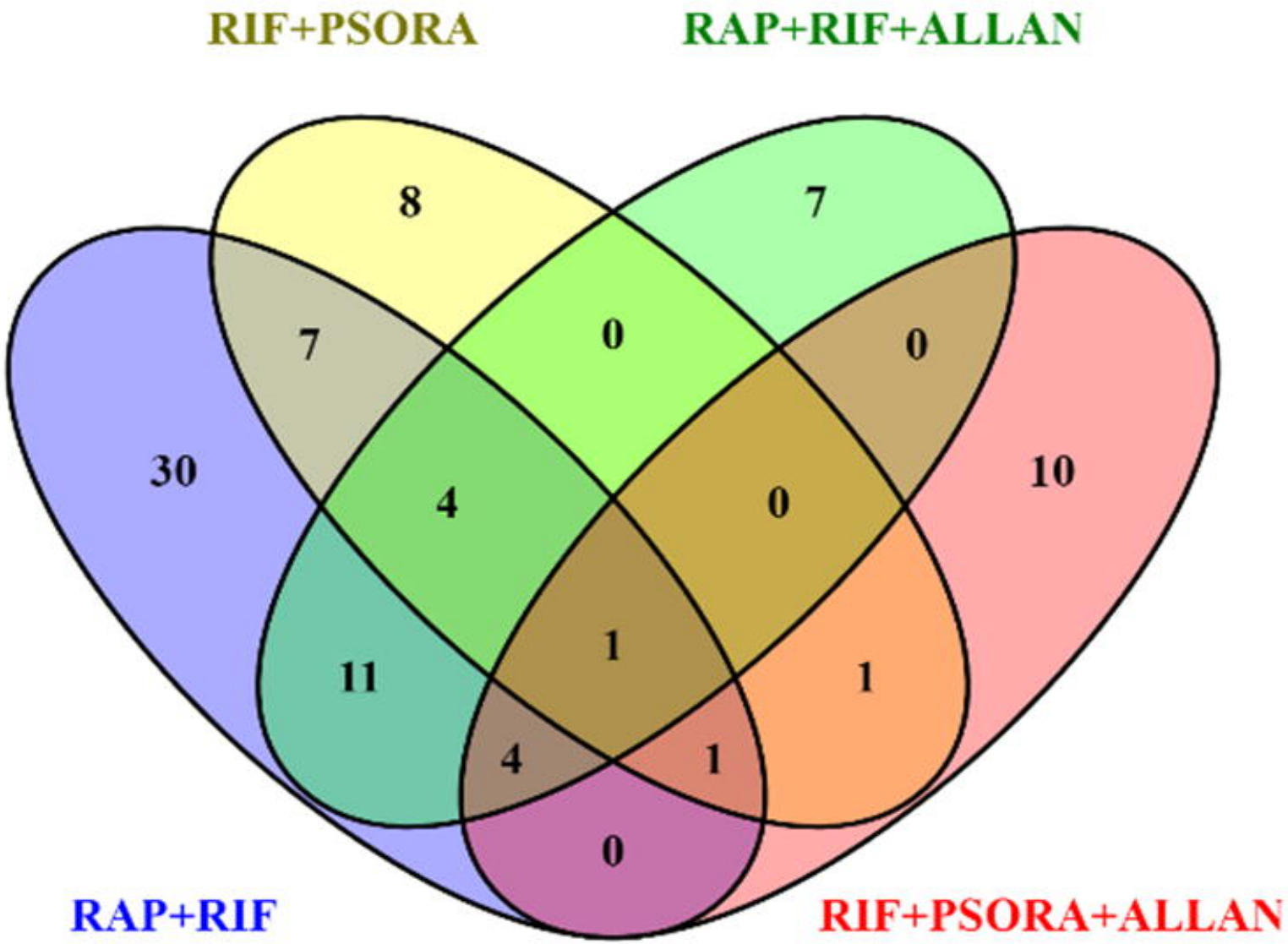
RIF+PSORA
RAP+RIF+ALLAN
8
7
7
0
0
30
4
0
10
11
1
1
4
1
0
RAP+RIF
RIF+PSORA+ALLAN

Figure 4

b

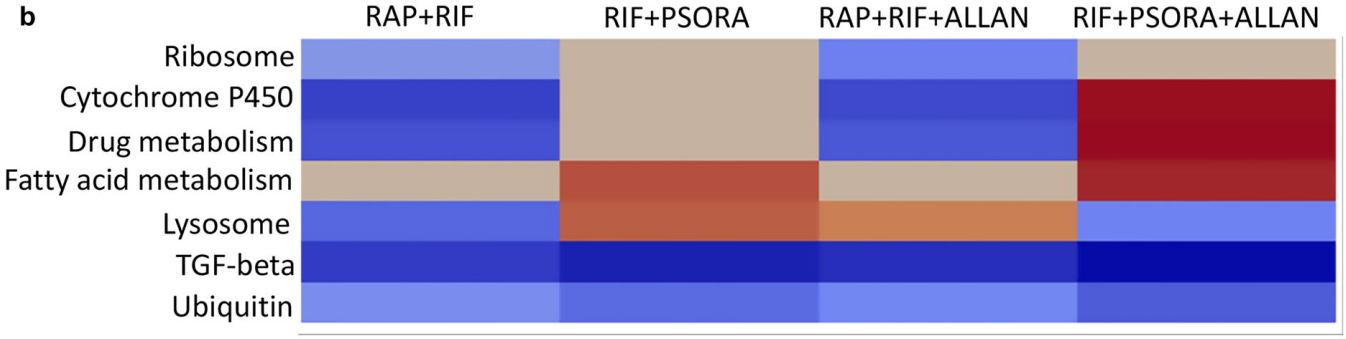
RAP+RIF
RIF+PSORA
RAP+RIF+ALLAN
RIF+PSORA+ALLAN
Ribosome
Cytochrome P450
Drug metabolism
Fatty acid metabolism
Lysosome
TGF-beta
Ubiquitin

Figure 4

c

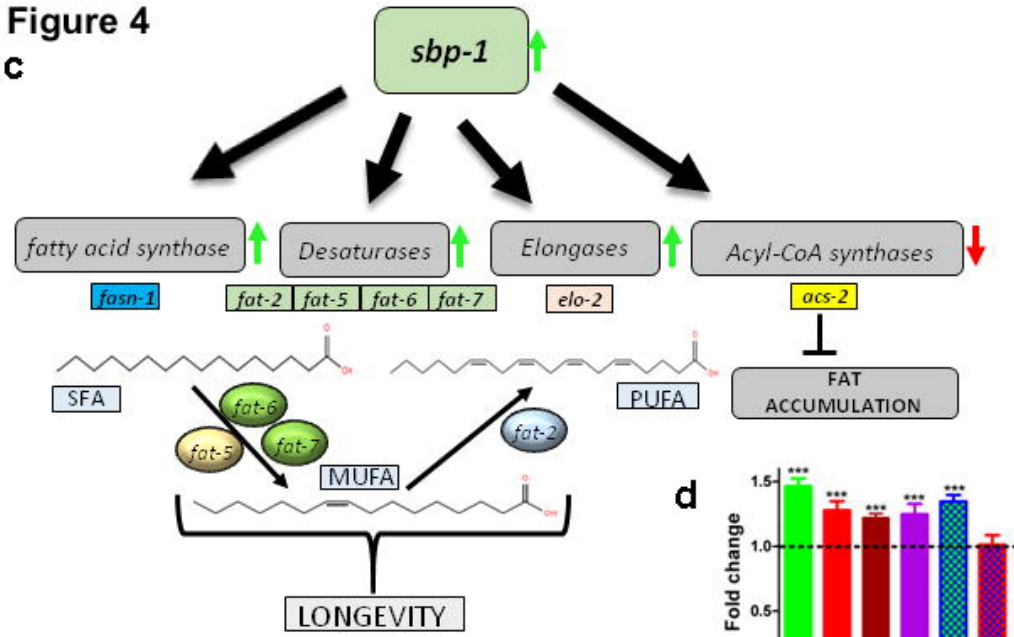

d

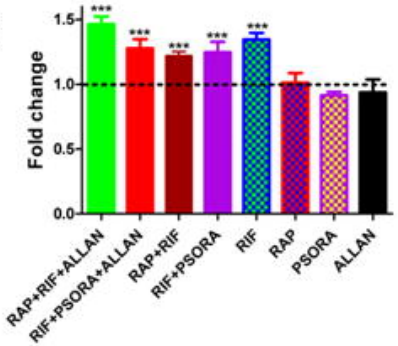

e

	MET	PSORA	RIF	RAP	ALLAN	RAP+MET	RAP+RIF	RIF+PSORA	RAP+RIF+ALLAN	RIF+PSORA+ALLAN
sbp-1	ns	ns	ns	ns	ns	ns	1.55	1.47	1.50	1.49
fasn-1	ns	ns	1.79	-1.22	ns	ns	1.52	ns	1.44	1.02
fat-2	ns	-1.85	-2.10	ns	ns	-2.65	-1.17	nS	ns	ns
fat-5	ns	-2.57	-2.10	ns	ns	-4.40	-1.74	nS	-1.11	ns
fat-6	ns	-1.38	ns	ns	ns	-2.08	ns	1.14	1.30	1.23
fat-7	ns	-2.12	-1.42	ns	ns	-2.55	-2.84	-2.72	-2.81	-2.48
elo-2	ns	ns	ns	ns	ns	ns	ns	ns	ns	ns
acs-2	ns	-2.37	-2.90	-2.13	ns	-2.76	-1.55	-1.35	-1.77	ns

f

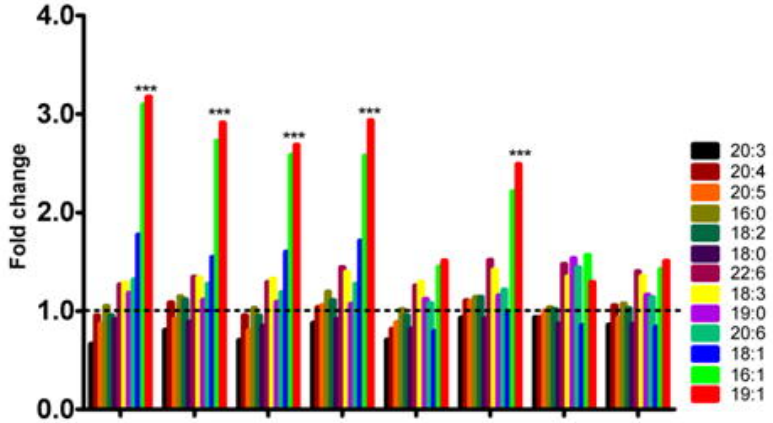

g

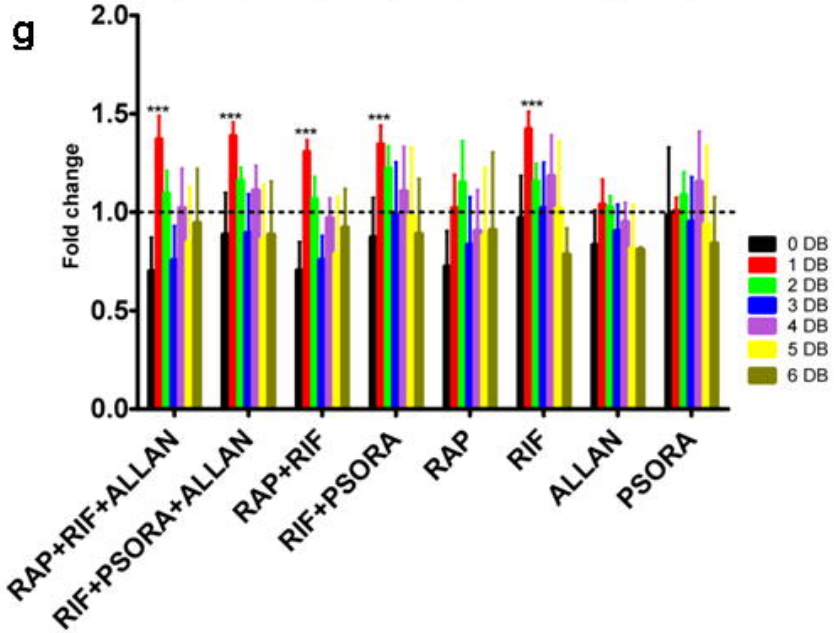

Figure 4

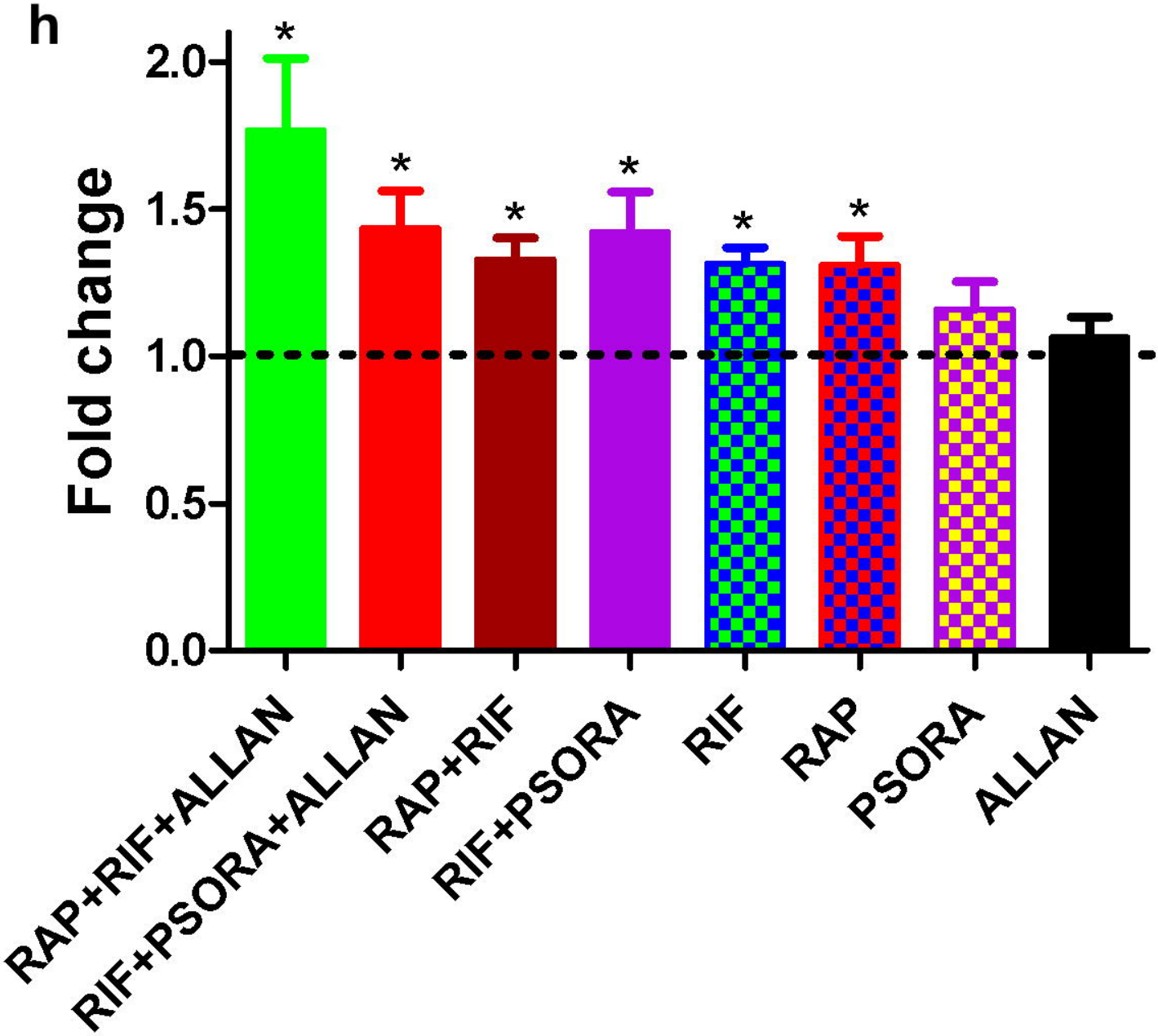
h
Fold change
2.0
1.5
1.0
0.5
0.0
*
RAP+RIF+ALLAN
RIF+PSORA+ALLAN
RAP+RIF
RIF+PSORA
RIF
RAP
PSORA
ALLAN

Figure 4
i

Drugs	PI±SE	DBI±SE	MUFA:PUFA
Control	138±4	172±4.5	1
PSORA	123±12	155±13	1.05±0.1
RIF	134±23	174±26	1.40±0.1
RAP	111±10	141±11	1.12±0.08
ALLAN	136±3.5	170±2	1.15±0.03
RAP+RIF	113±14	159±14.5	1.48±0.16
RIF+PSORA	133±13.5	183±15	1.34±0.14
RAP+RIF+ALLAN	120±12	171±15	1.50±0.1
RIF+PSORA+ALLAN	127±17	175±20	1.45±0.17

Figure 4

j

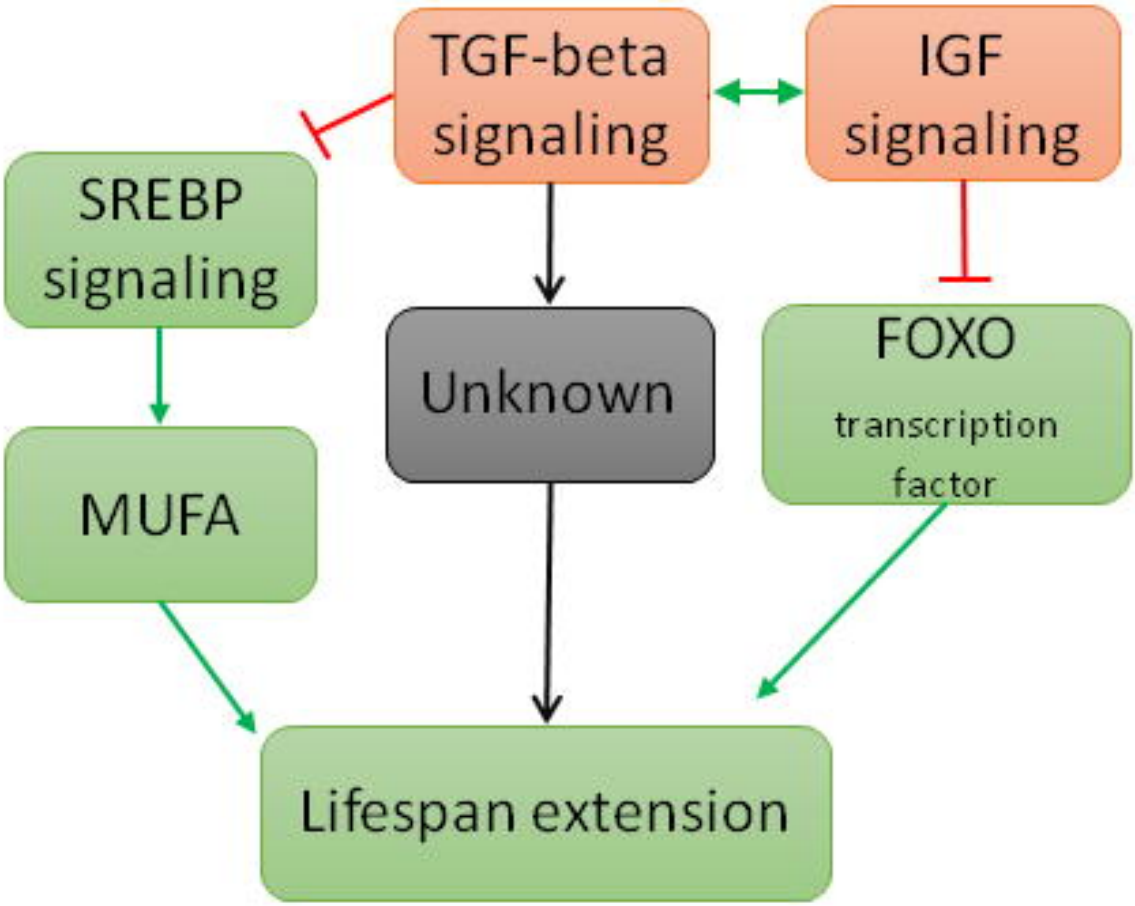
TGF-beta signaling
IGF signaling
SREBP signaling
Unknown
FOXO transcription factor
MUFA
Lifespan extension

Figure 5

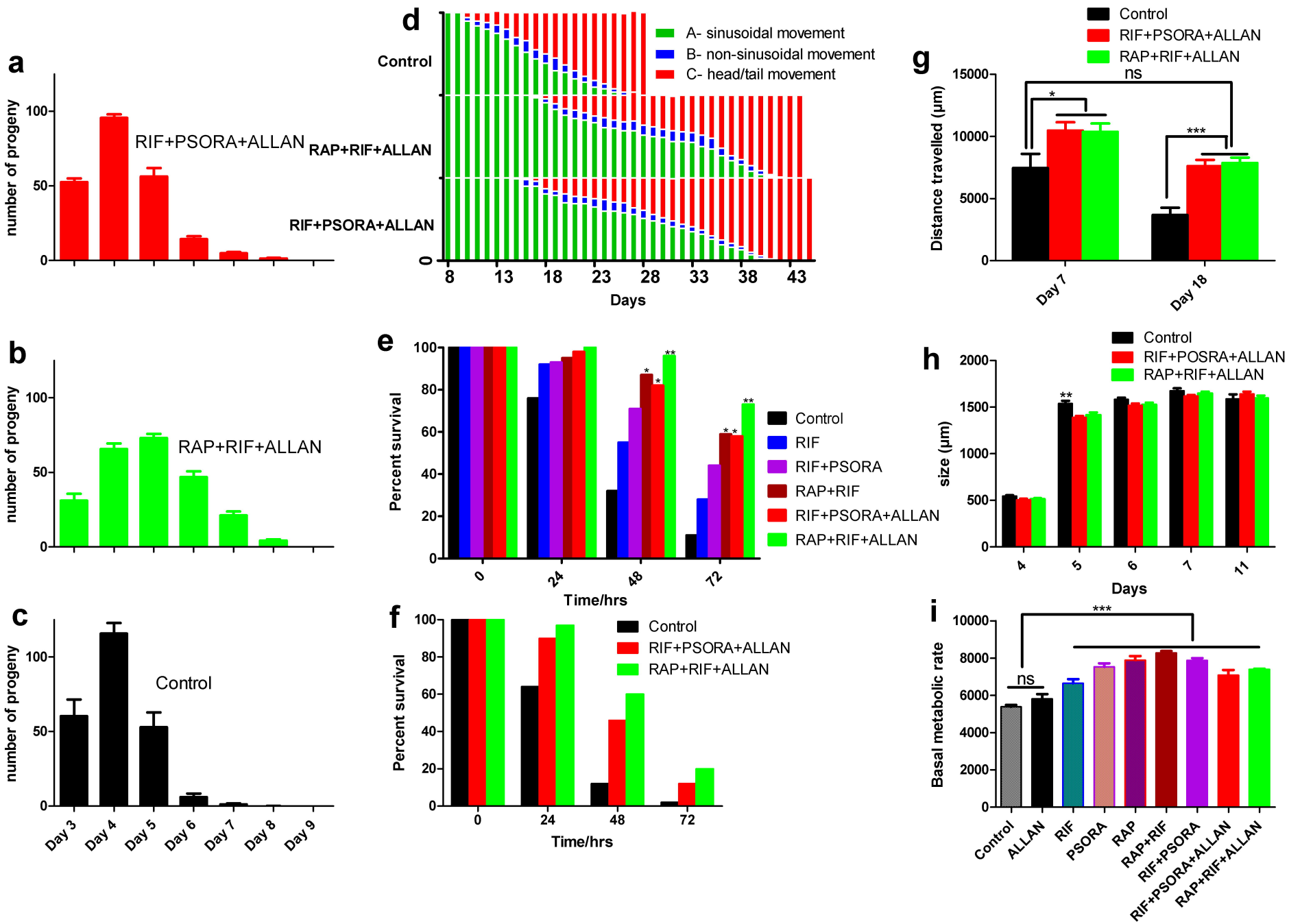
a
number of progeny
RIF+PSORA+ALLAN
b
number of progeny
RAP+RIF+ALLAN
c
number of progeny
Control
Day 3
Day 4
Day 5
Day 6
Day 7
Day 8
Day 9
d
Control
RAP+RIF+ALLAN
RIF+PSORA+ALLAN
A- sinusoidal movement
B- non-sinusoidal movement
C- head/tail movement
Days
e
Percent survival
Time/hrs
Control
RIF
RIF+PSORA
RAP+RIF
RIF+PSORA+ALLAN
RAP+RIF+ALLAN
f
Percent survival
Time/hrs
Control
RIF+PSORA+ALLAN
RAP+RIF+ALLAN
g
Control
RIF+PSORA+ALLAN
RAP+RIF+ALLAN
Distance travelled (µm)
ns
Day 7
Day 18
h
Control
RIF+POSRA+ALLAN
RAP+RIF+ALLAN
size (µm)
Days
i
Basal metabolic rate
ns
Control
ALLAN
RIF
PSORA
RAP
RAP+RIF
RIF+PSORA
RIF+PSORA+ALLAN
RAP+RIF+ALLAN

Figure 6

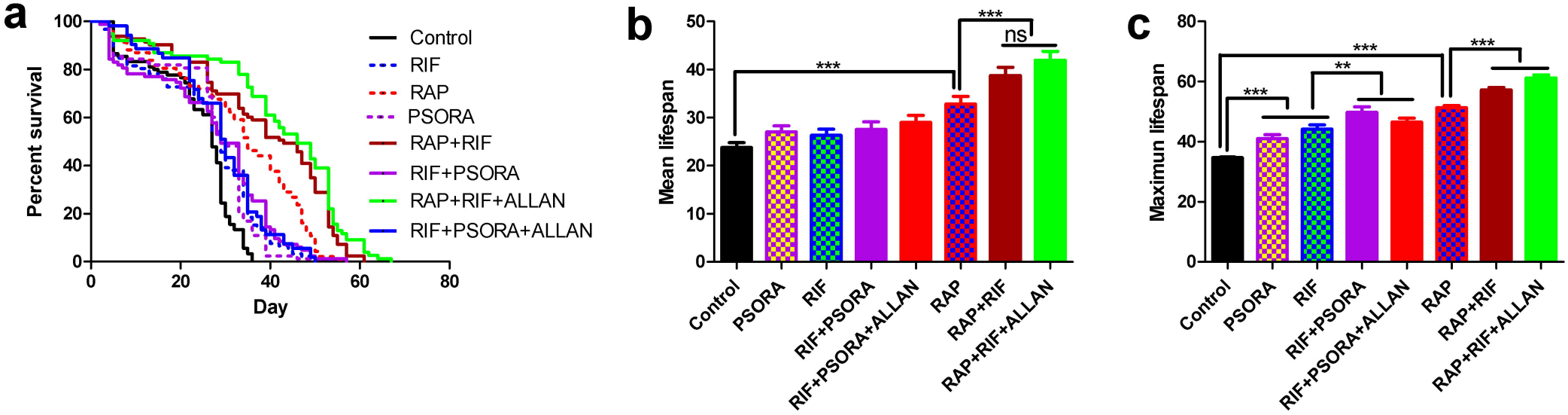
a
Percent survival
Day
Control
RIF
RAP
PSORA
RAP+RIF
RIF+PSORA
RAP+RIF+ALLAN
RIF+PSORA+ALLAN
b
Mean lifespan
***
ns
Control
PSORA
RIF
RIF+PSORA
RIF+PSORA+ALLAN
RAP
RAP+RIF
RAP+RIF+ALLAN
c
Maximun lifespan
***
**

Extended data: Supplementary figures and figure legends

Figure S1

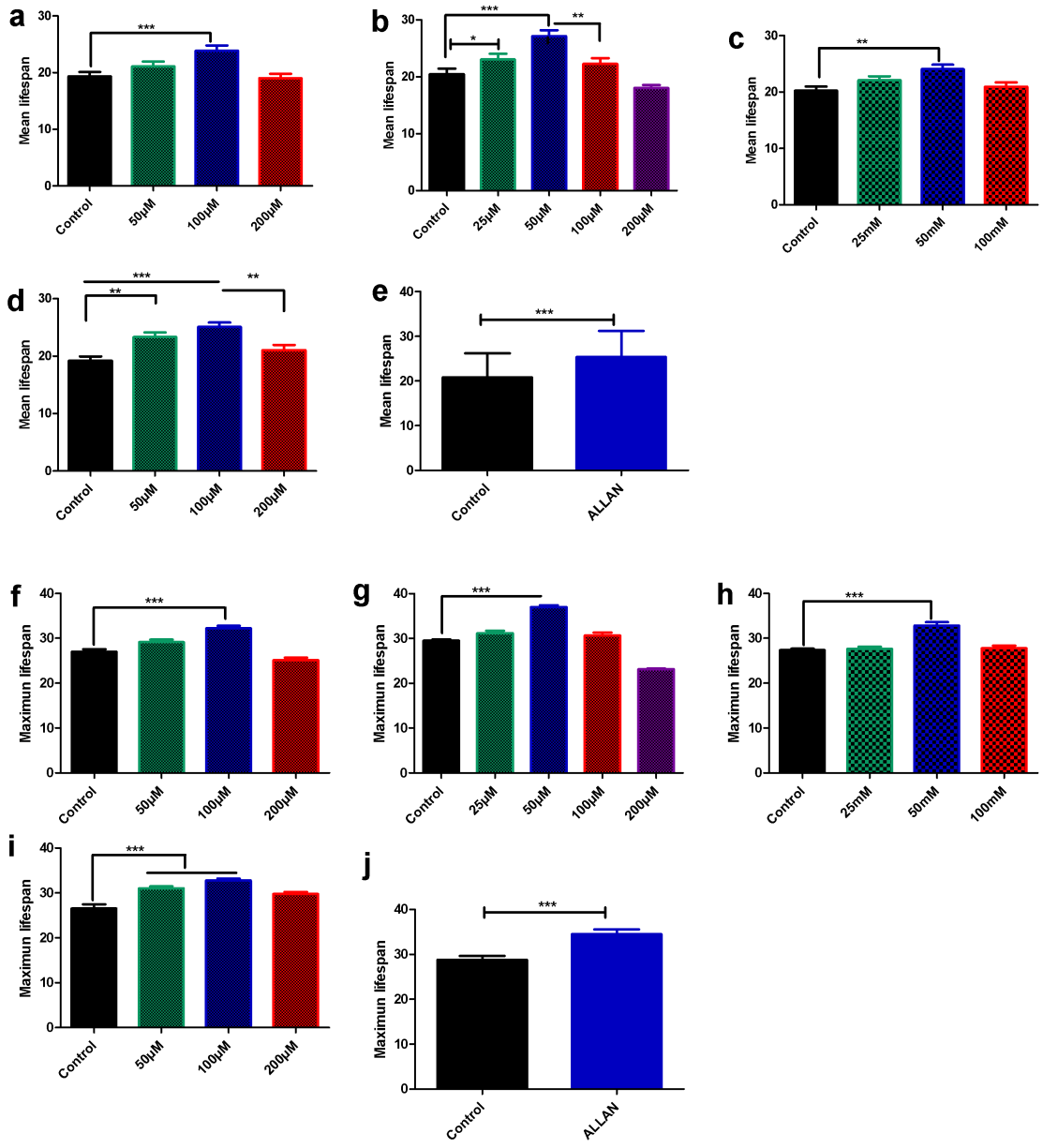

Figure S1: Mean and Maximum lifespan of worms treated with ranges of doses of different drugs. Drug treatment started at day 4 and continued until all worms died. Worms were transferred to fresh plate every day 3-4 days. (a-e) Mean and (f-j) Maximum lifespan of single drug treatments supplementary to figure 1. **a** and **f** – RAP, **b** and **g** – RIF, **c** and **h** – MET, **d** and **i** – PSORA, **e** and **j** – ALLAN (Mean ± SE) ***P < 0.0001, **P < 0.001, *P < 0.01

Figure S2

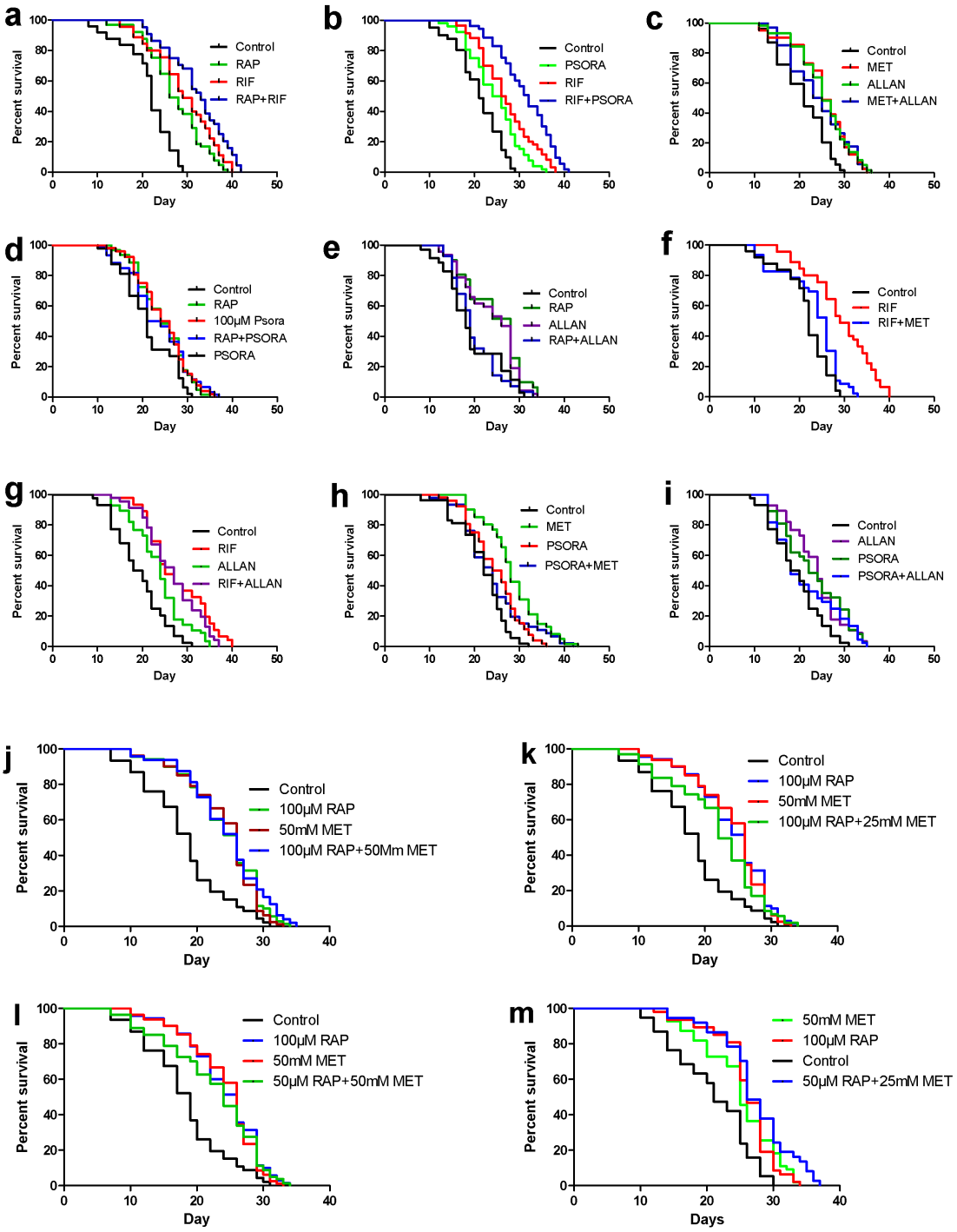
a
Percent survival
Day
Control
RAP
RIF
RAP+RIF
b
Percent survival
Day
Control
PSORA
RIF
RIF+PSORA
c
Percent survival
Day
Control
MET
ALLAN
MET+ALLAN
d
Percent survival
Day
Control
RAP
100μM Psora
RAP+PSORA
PSORA
e
Percent survival
Day
Control
RAP
ALLAN
RAP+ALLAN
f
Percent survival
Day
Control
RIF
RIF+MET
g
Percent survival
Day
Control
RIF
ALLAN
RIF+ALLAN
h
Percent survival
Day
Control
MET
PSORA
PSORA+MET
i
Percent survival
Day
Control
ALLAN
PSORA
PSORA+ALLAN
j
Percent survival
Day
Control
100μM RAP
50mM MET
100μM RAP+50Mm MET
k
Percent survival
Day
Control
100μM RAP
50mM MET
100μM RAP+25mM MET
l
Percent survival
Day
Control
100μM RAP
50mM MET
50μM RAP+50mM MET
m
Percent survival
Days
50mM MET
100μM RAP
Control
50μM RAP+25mM MET

Figure S2 - cont

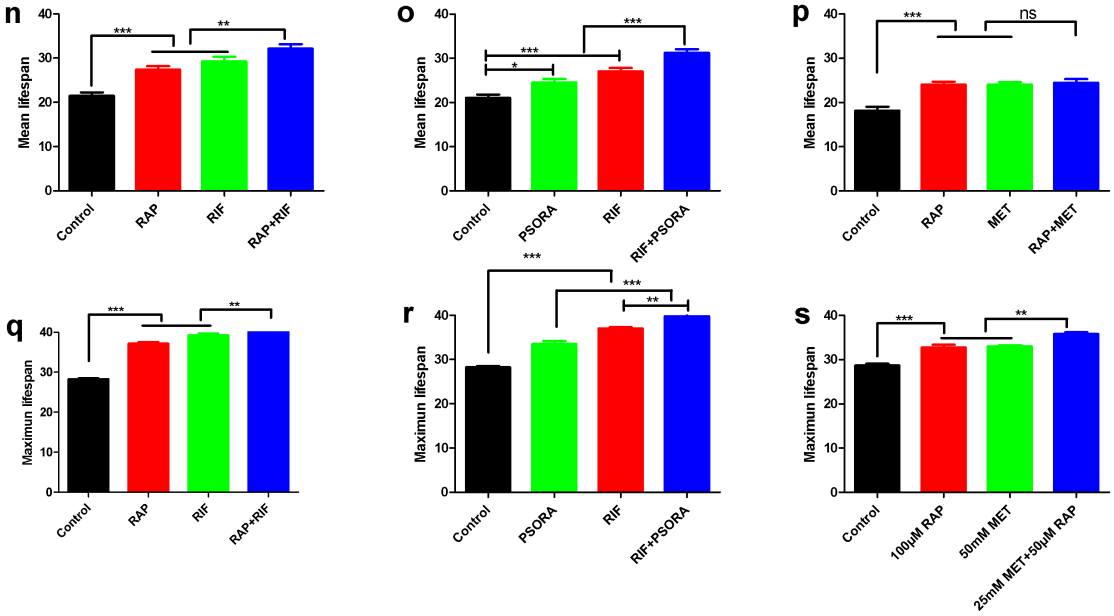

Figures S2 lifespan comparison of double combinations supplementary for figure 2. **a-i,** survival curve for all 10 possible combinations of five drugs at their respective optimal dose except RAP+MET. **j-m,** all possible combinations of RAP and MET at their optimal and half-optimal doses. **n-p**, Mean lifespan of representative dual combinations, (Mean ± SE) **q-s**, maximum lifespan of representative dual combinations, (Mean ± SE). ***P < 0.0001, **P < 0.001, *P < 0.01

Figure S3

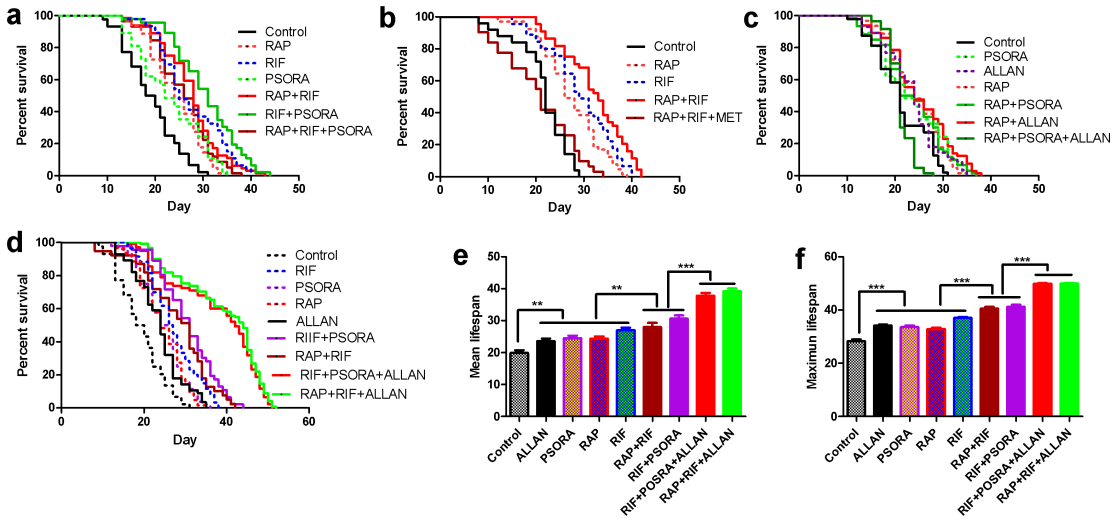

Figures S3 lifespan comparison of triple combinations supplementary for figure 2. **a**, RAP+RIF+PSORA did not show further benefit compared to the dual synergistic combinations RAP+RIF and RIF+PSORA. **b**, RAP+RIF+MET is toxic compared to RAP+RIF. More than 50 worms per condition.. **c**, RAP+PSORA+ALLAN did not show further benefit compared to single drug constituents. **d**, RAP+RIF+ALLAN and RIF+PSORA+ALLAN resulted in a significant lifespan extension compared to RAP+RIF and RIF+PSORA respectively. **e**, Mean and **f**, Maximum lifespan of figure d showed a monotonic increase from single drugs to double and triple combinations. ***P<0.0001, **P<0.001, *P<0.01.

Figure S4

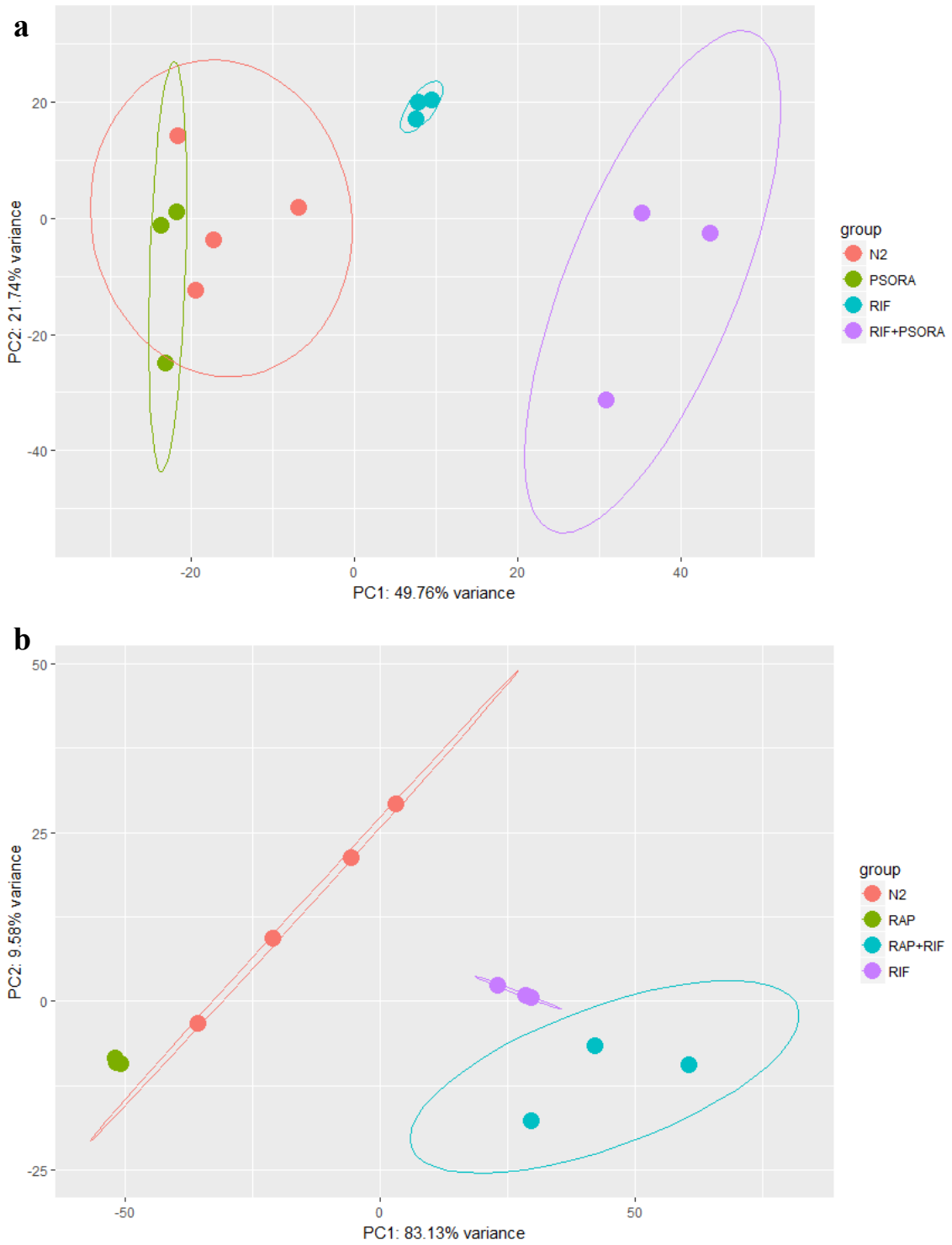
a
20
0
-20
-40
PC2: 21.74% variance
-20
0
20
40
PC1: 49.76% variance
group
N2
PSORA
RIF
RIF+PSORA
b
50
25
0
-25
PC2: 9.58% variance
-50
0
50
PC1: 83.13% variance
group
N2
RAP
RAP+RIF
RIF

Figure S4 - cont

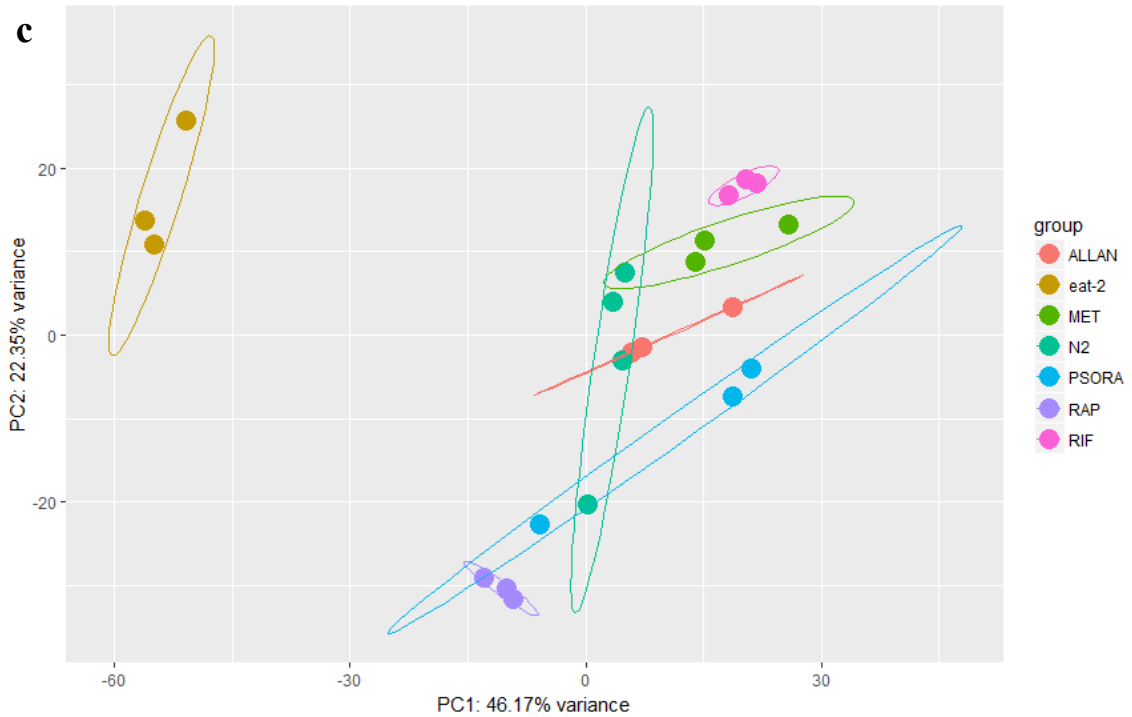

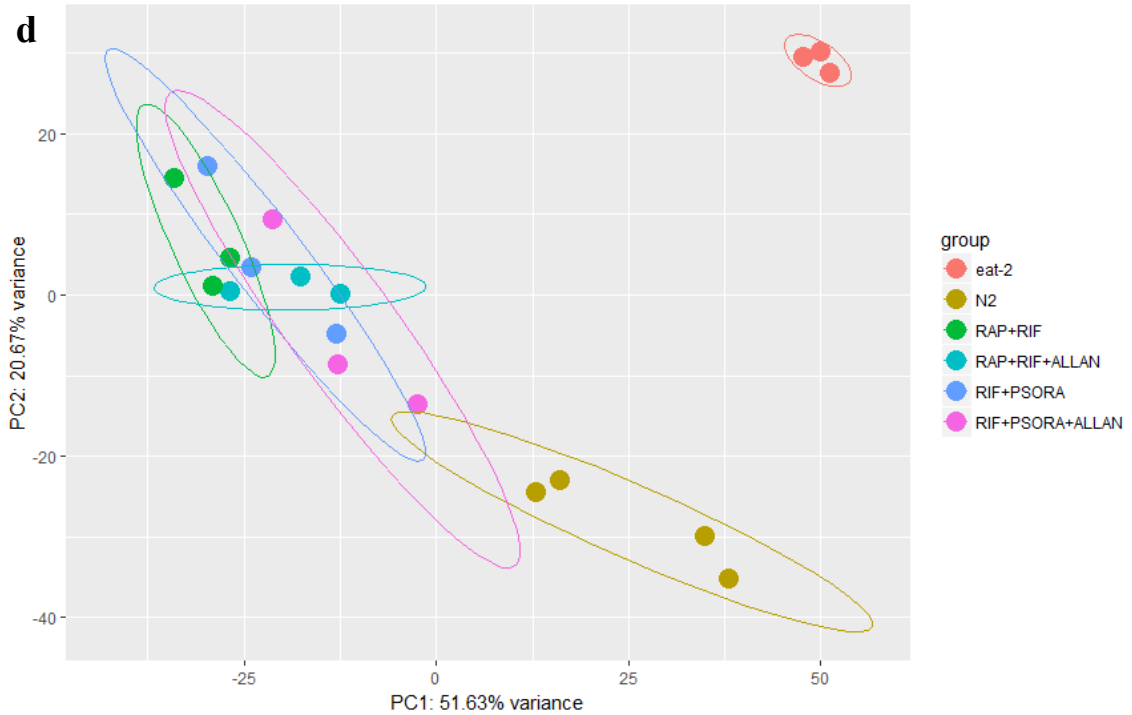

Figure S4 - cont

Figure S4. 2D Principle component analysis (PCA), Transcriptome profile based on the differentially expressed genes of each drug and drug combination projected onto top two PCs. a, 2D PCA of PSORA, RIF and their combination showed that the combination transcriptome profile is different from single drugs. Because the single drugs and the combinations were sequenced in two different lanes, we used the N2 untreated controls of both lanes. **b**, as in **a** for RAP and RIF. **c**, similar to the 3D PCA, RAP, RIF and PSORA were well separated with 2D PCA. All single drugs were separated from eat-2. **d**, all synergistic combinations are well separated with N2 control and eat-2, whereas they are not separated from each other. This could show that they may have the same mechanism of synergistic lifespan extension.

Figure S5

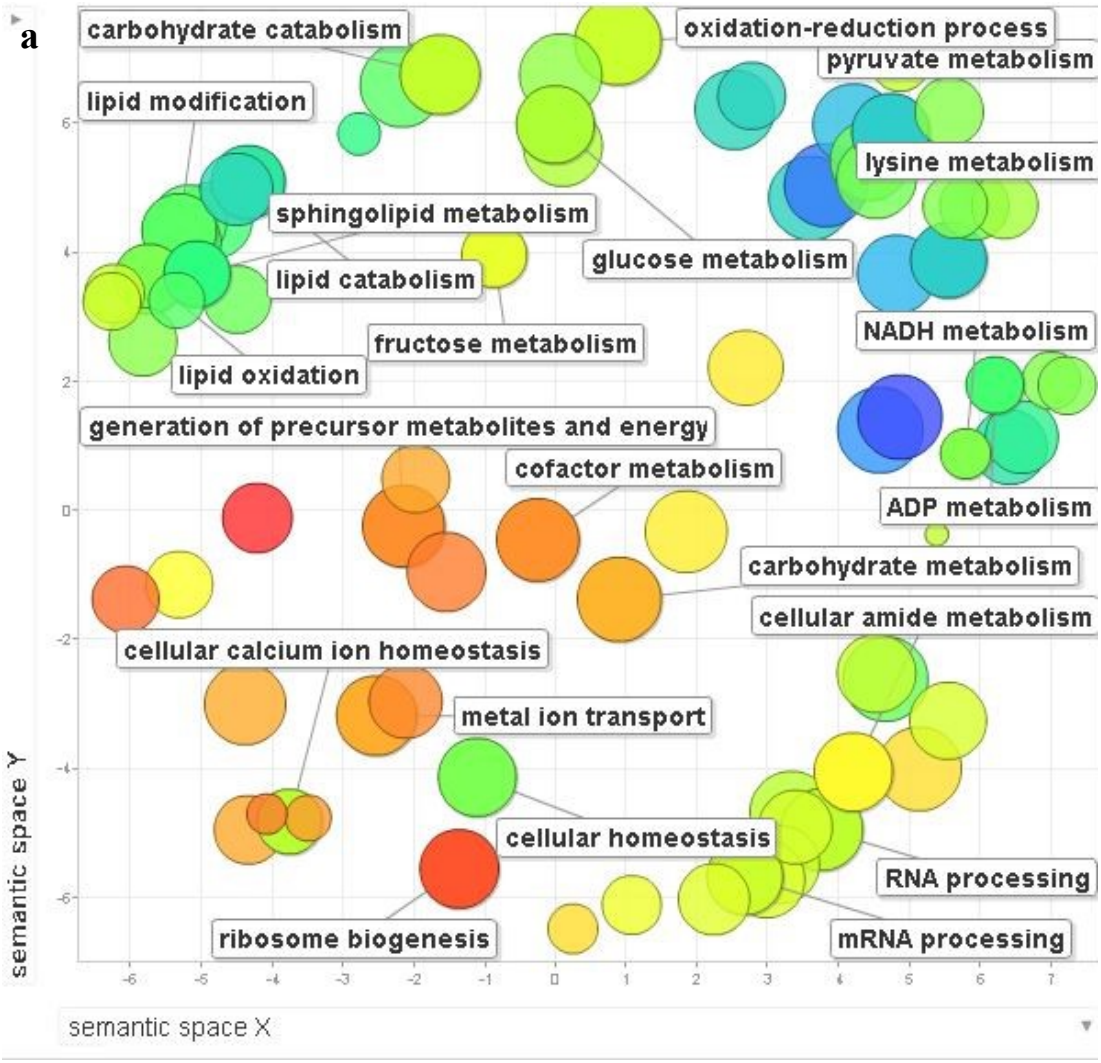
a
carbohydrate catabolism
oxidation-reduction process
pyruvate metabolism
lipid modification
lysine metabolism
sphingolipid metabolism
glucose metabolism
lipid catabolism
NADH metabolism
fructose metabolism
lipid oxidation
generation of precursor metabolites and energy
cofactor metabolism
ADP metabolism
carbohydrate metabolism
cellular amide metabolism
cellular calcium ion homeostasis
metal ion transport
cellular homeostasis
RNA processing
ribosome biogenesis
mRNA processing
semantic space Y
semantic space X

Figure S5 - cont

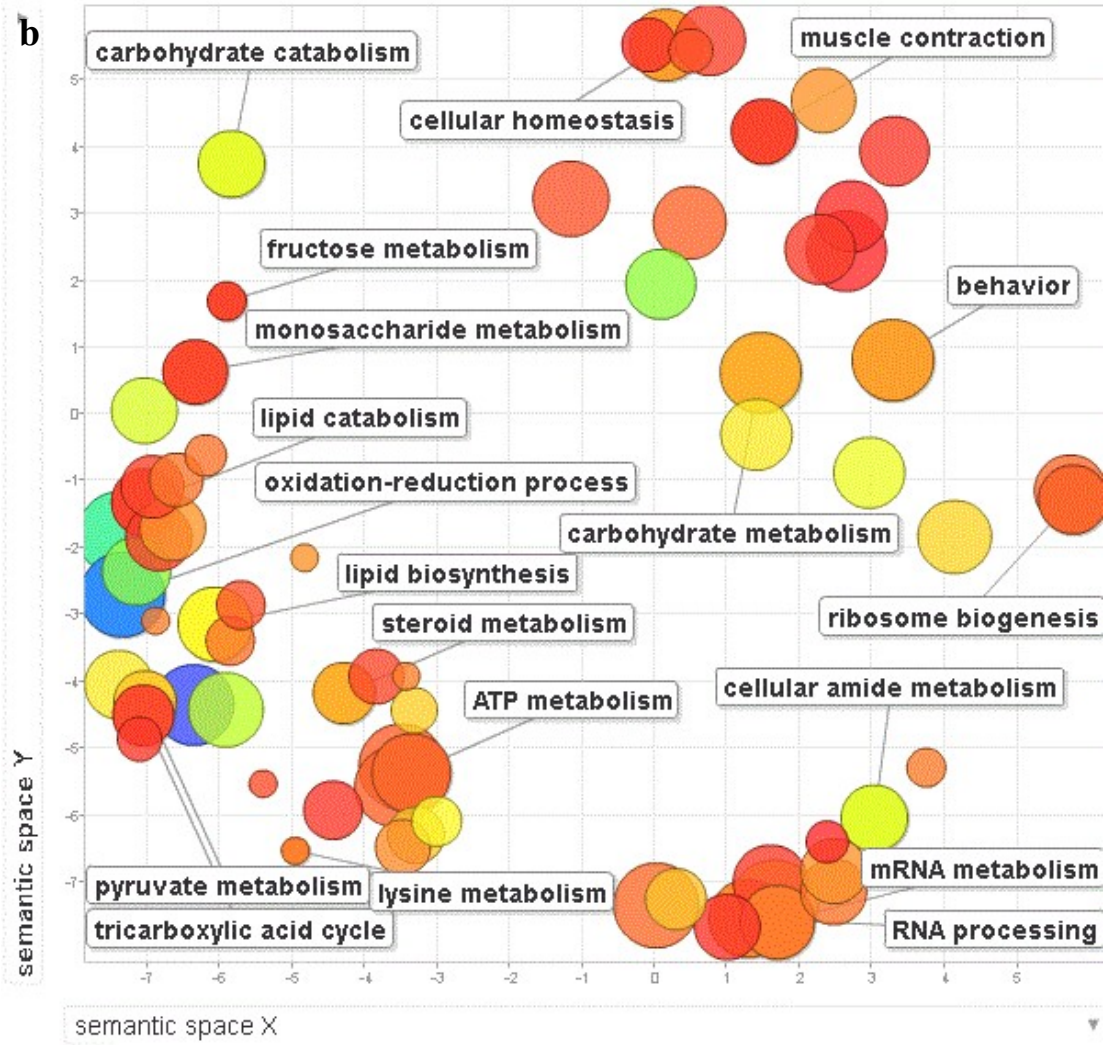

Figure S5 GO terms enriched by synergistic triple drug combinations determined by Cytoscape[70] and summarized by Revigo[71]. Differentially expressed genes (|LFC| >= 1, P value < 0.05) for each conditions were used as an input for GO term analysis. both **a**, RIF+PSORA+ALLAN, and **b**, RAP+RIF+ALLAN mainly targets metabolic pathways. (P value < 0.05, term enrichment > 1.5)

Figure S6

a

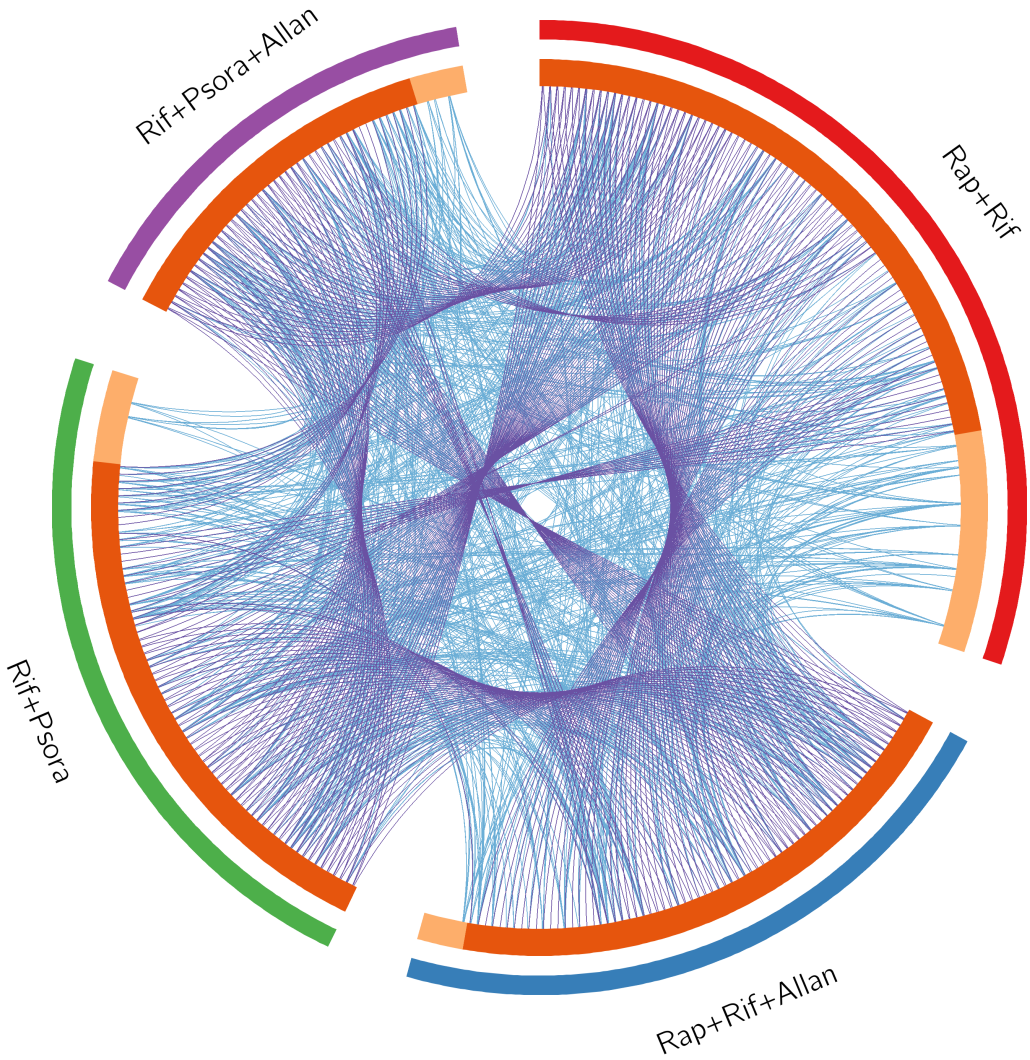

Figure S6 - cont

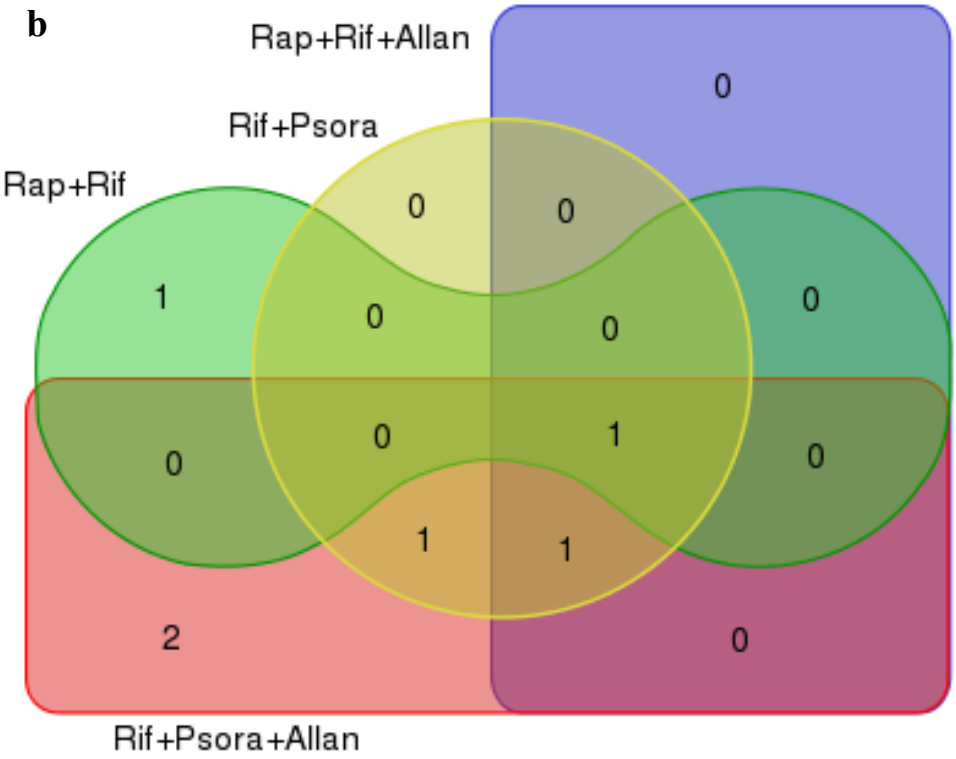

Figure S6 Gene signature and pathway overlap for synergistic combinations: supplementary for figure 5. a, DGE and GO term overlap among synergistic combinations. Purple line links identical genes whereas blue line links different gene that grouped into similar GO terms. **b**, Venn diagram of pathways enriched in synergistic combinations using eat-2 transcriptome as a background. Only TGF-beta was commonly enriched in all synergistic combinations.

Figure S7

a

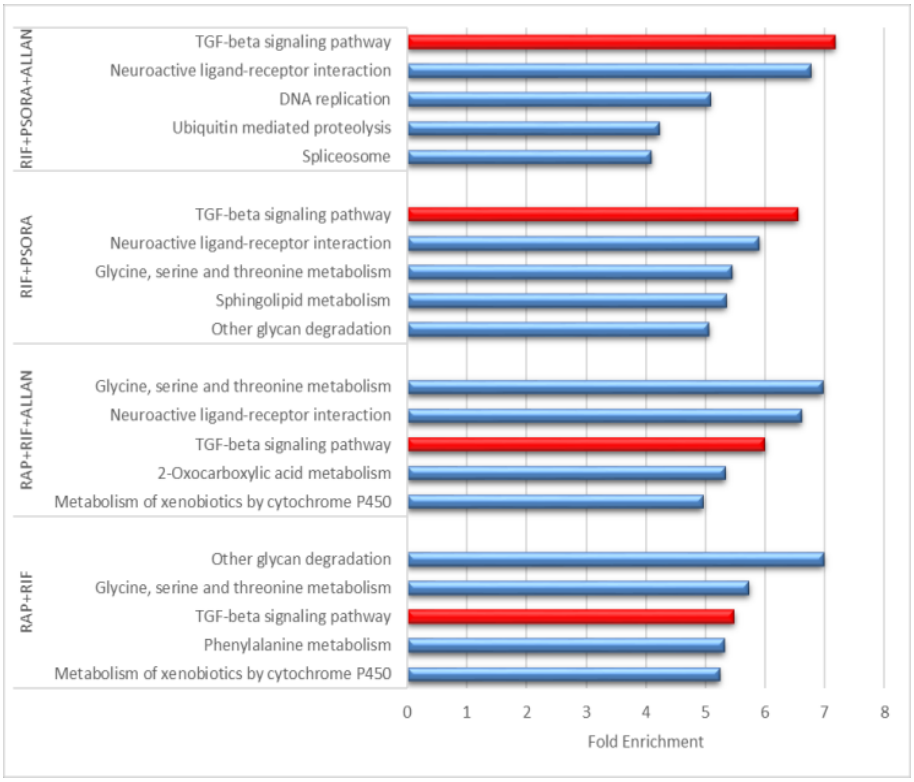
RIF+PSORA+ALLAN
TGF-beta signaling pathway
Neuroactive ligand-receptor interaction
DNA replication
Ubiquitin mediated proteolysis
Spliceosome
RIF+PSORA
TGF-beta signaling pathway
Neuroactive ligand-receptor interaction
Glycine, serine and threonine metabolism
Sphingolipid metabolism
Other glycan degradation
RAP+RIF+ALLAN
Glycine, serine and threonine metabolism
Neuroactive ligand-receptor interaction
TGF-beta signaling pathway
2-Oxocarboxylic acid metabolism
Metabolism of xenobiotics by cytochrome P450
RAP+RIF
Other glycan degradation
Glycine, serine and threonine metabolism
TGF-beta signaling pathway
Phenylalanine metabolism
Metabolism of xenobiotics by cytochrome P450
0
1
2
3
4
5
6
7
8
Fold Enrichment

Figure S7 - cont

b

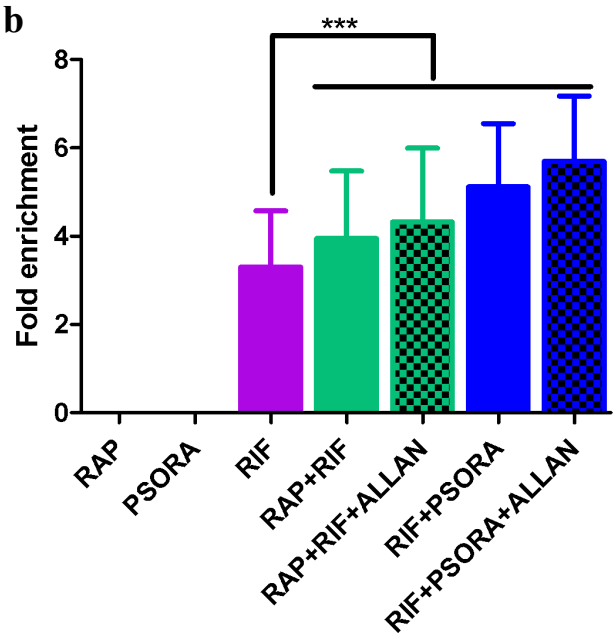

c

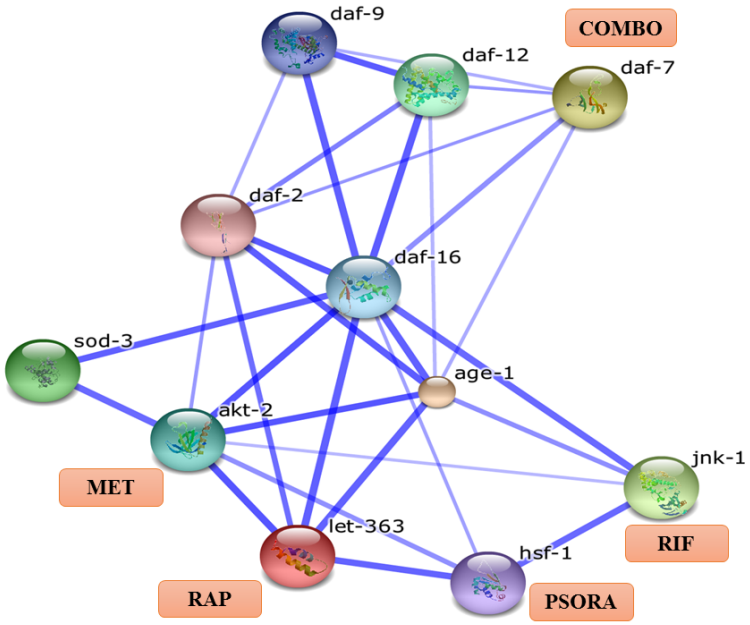

Figure S7 - cont

d

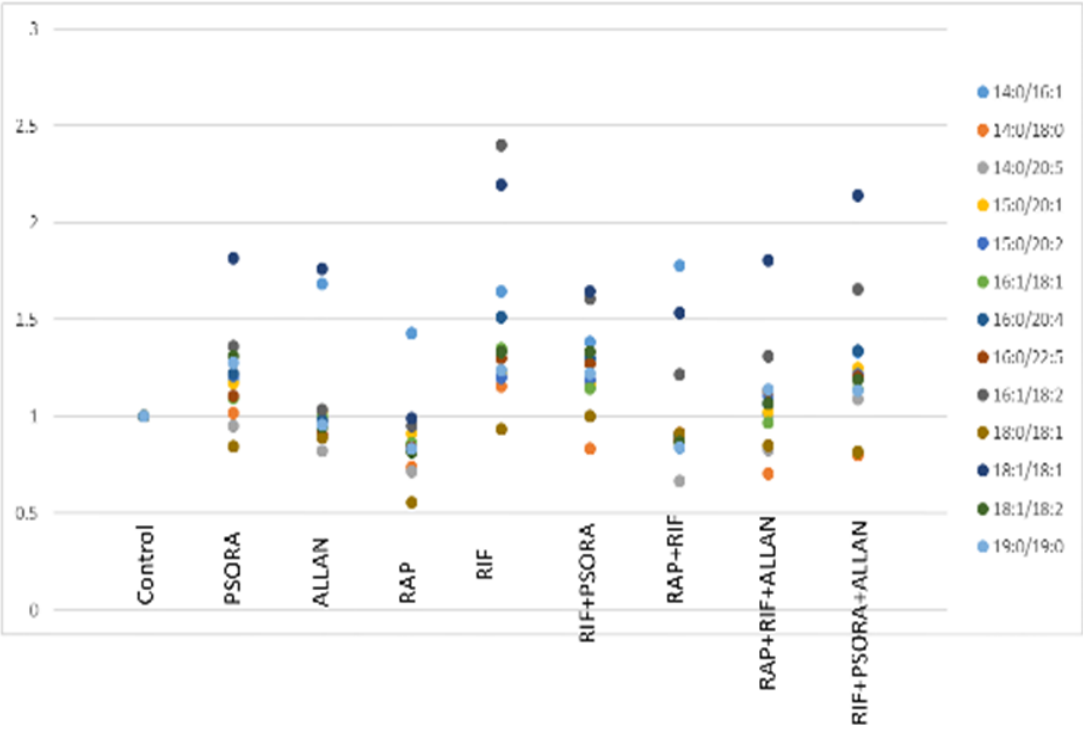

Figure S7 TGF-beta pathway is significantly enriched in the synergistic drug combinations differentially expressed genes. a, Top five pathways enriched in the down regulated genes of the four synergistic drug combinations. All synergistic combinations consistently enrich TGFβ. **b**, Pathways enriched in N2 animals treated with synergistic drug combinations relative to untreated eat-2 worms. All synergistic combinations consistently enrich TGFβ. **c**, fold enrichment of TGFβ in all single drugs and synergistic combinations. From single drugs, only RIF enriched TGFβ. All the four synergistic combinations resulted in a significant enrichment of TGFβ compared to RIF. **d**, protein-protein interaction drawn by STRING[72] showed that TGFβ/daf-7 has an interaction with daf-2 and daf-16 as well as the lipid metabolism regulators daf-9 and daf-12. Thickness of the edge indicates strength of data support for the specific interaction. **e**, A stacked dotplot representation of phosphatidylethanolamine class showing an increase in monounsaturated containing species, 2500 worms per condition (Mean ± SD) *P<0.01, **P<0.001, ***P<0.000.

Figure S8

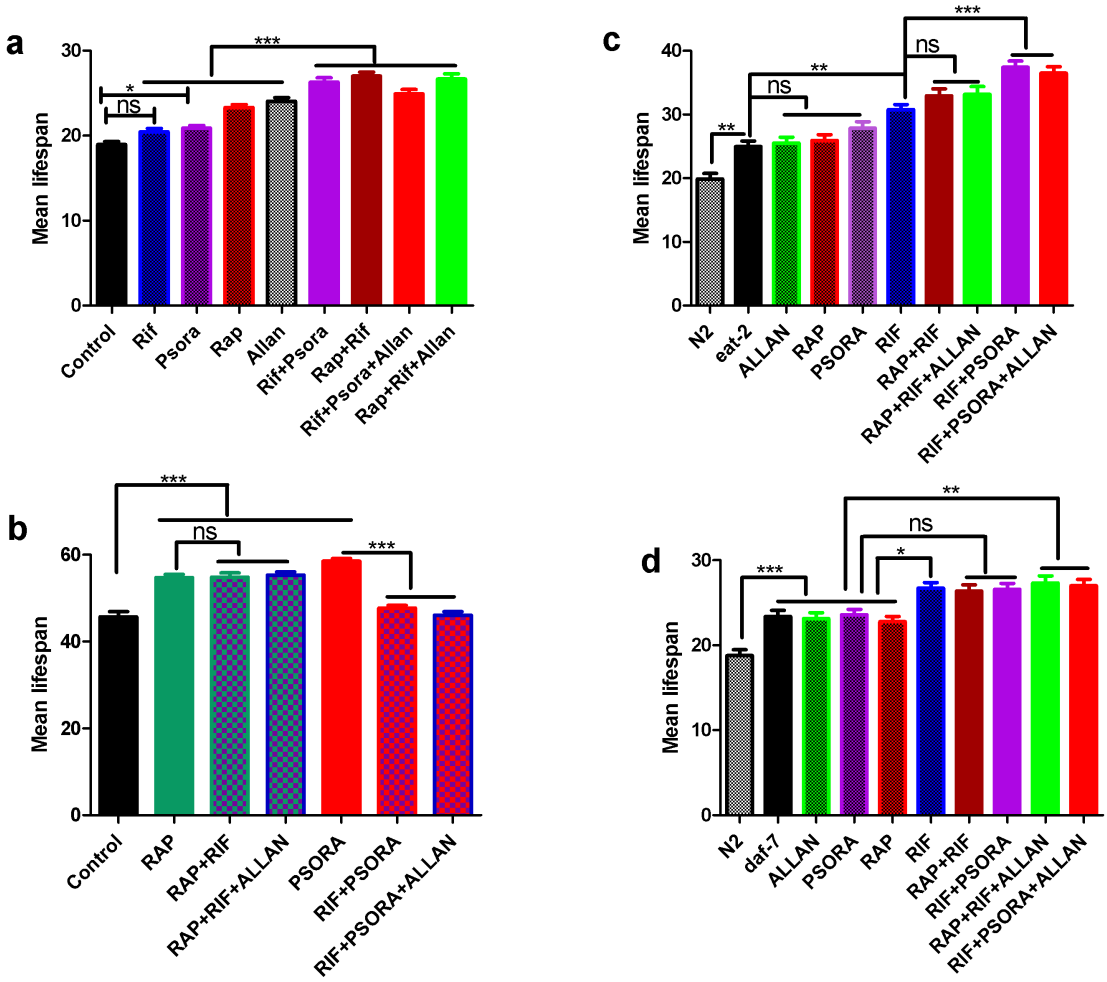

Figure S8 Mean lifespan on daf-16, eat-2, daf-2 and daf-7 mutants treated with single drugs and drug combinations. **a**, Dual combinations RAP+RIF and RIF+PSORA showed synergy in daf-16 where as the triple combinations RAP+RIF+ALLAN and RIF+PSORA+ALLAN did not result in significant difference from their respective synergistic dual combinations. **b**, All synergistic combinations did not show synergy in daf-2 mutant worms. **c**, Only RIF+PSORA showed synergy in eat-2 mutants. **d**, The triple combinations showed further lifespan extension compared to single drugs but none of the four combinations show synergy in daf-7 mutants. Supplementary for figure 4. At least 50 worms per condition. ***P<0.0001, **P<0.001, *P<0.01.

Figure S9

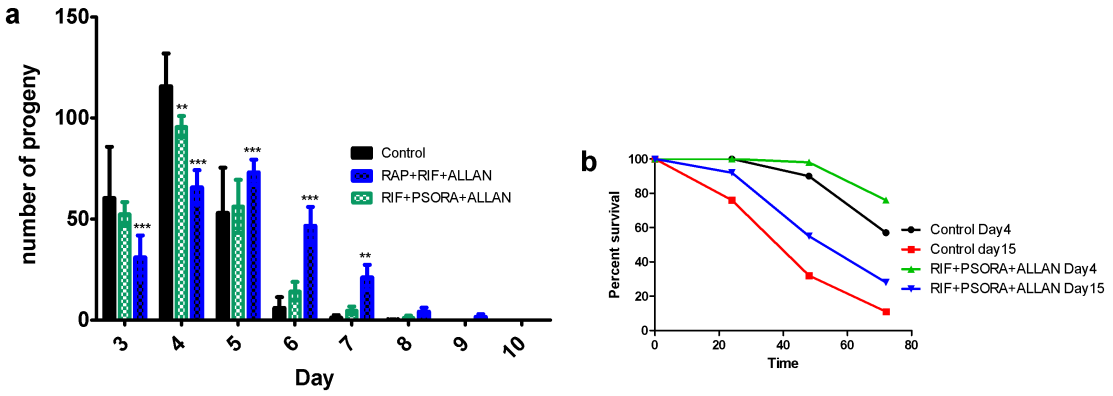

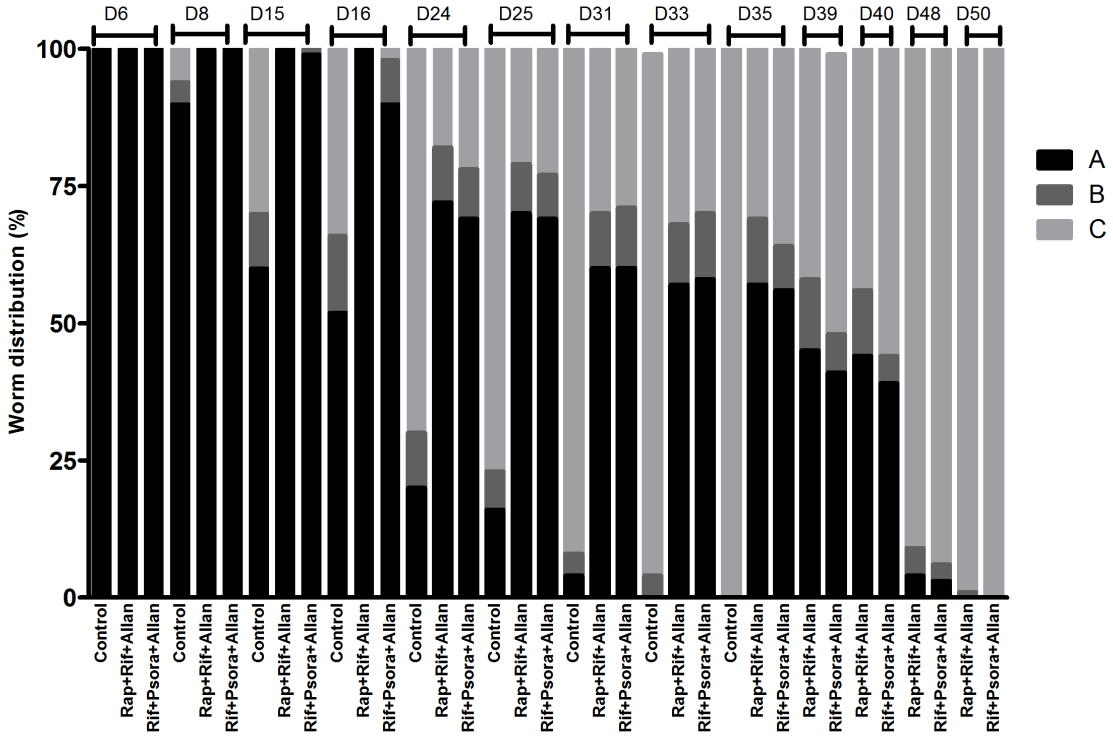

Figure S9 Health span and tradeoffs supplementary for figure 3. **a**, Drug synergies extended reproductive period. 10 worms per condition**. b,** Heat shock stress, RIF+PSORA+ALLAN improves heat shock stress resistance both at young, day 4, worms and older, day 15, worms **c**, Health span scoring at different age. At all ages from young to old drug synergy treated worms have better health span than their respective age matched controls. ***P<0.0001, **P<0.001, *P<0.01.

Figure S10

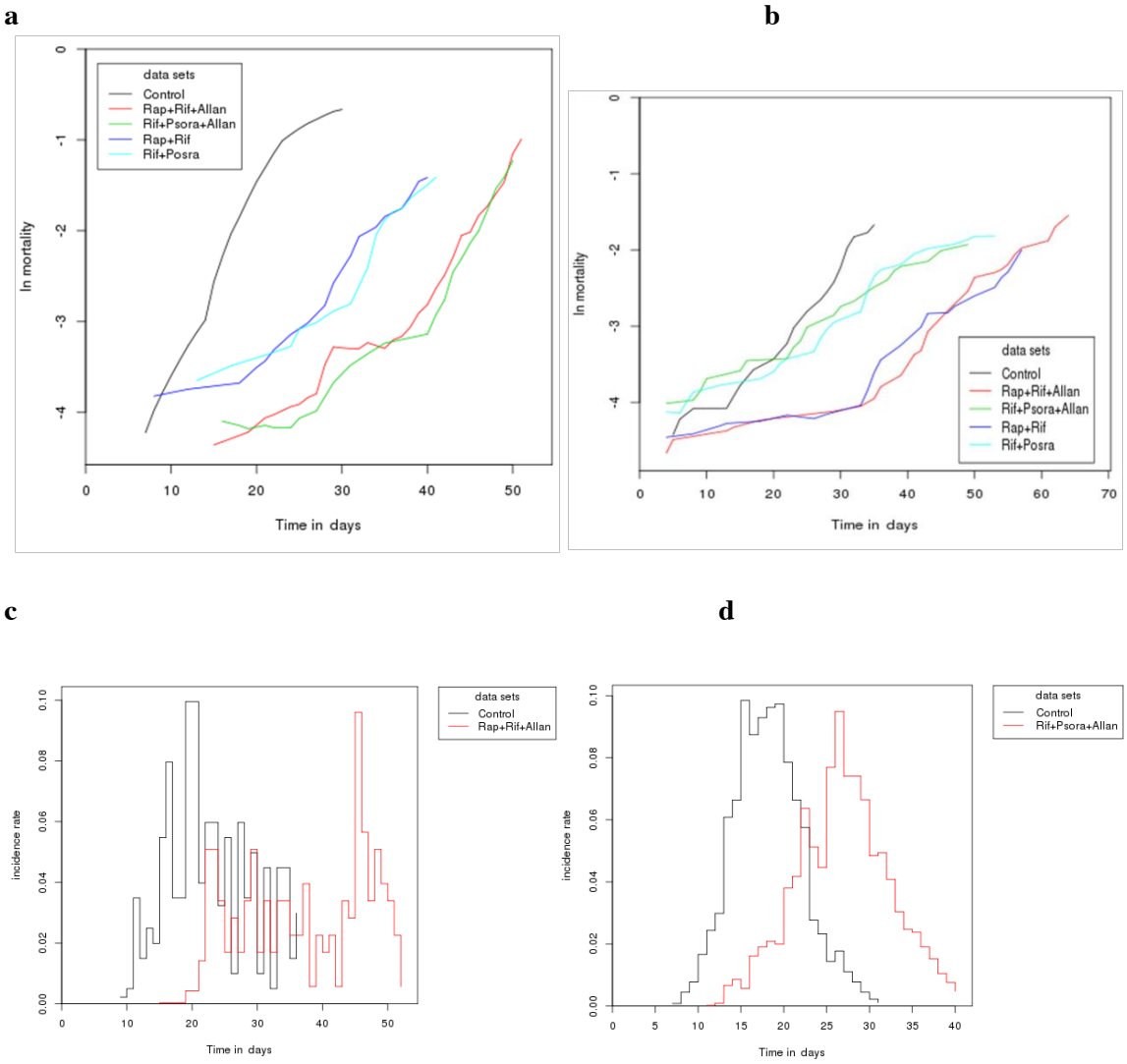

Figure S10. Drug synergy slows mortality rate and delays death incidence rate; **a**, Both the dual and triple synergistic combinations slow the rate of mortality of wild type N2 worms. **b**, The triple combinations RAP+RIF+ALLAN and RIF+PSORA+ALLAN slows mortality rate in Drosophila Melanogaster. **c**, Incident rate of deaths in control cohorts compared to treated cohorts for RAP+RIF+ALLAN and **d**, RIF+PSORA+ALLAN treatment. Both treatments delay peak of incidence rate of death in worms.

Table S1 Drug selection based on ageing pathways

Drugs	Proposed pathway	References
Rapamycin	mTORC1	[1-3]
Rifampicin	JNK	[4]
Metformin	Mitohormesis, microbial folate metabolism, AMPK	[5-7]
Psora-4	K-channel blocker, Hormesis	[8]
Allantoin	CR mimetic	[9]
Torin-1	mTORC2	None
Aspirin	AMPK/DAF-16, Hormesis	[10, 11]
Mianserin	CR memetic	[12, 13]
Loxapine Succinate	Unknown	[8]
Juglone	ROS	[14]
cAMP	CR mimetic	[15]

Table S2 Summary of Lifespan Studies, all lifespan studies, at least two biological replicates.

Exp no	Strain	Conditions	No. Animals	Mean lifespan	% Change	P-value vs control	Maximum lifespan	% Change	P-value vs control
1	N2	Psora-4	83	25	30.5	***	33	23.5	***
		Control	79	19			26.5		
2		Rifampicin	75	27	32.5	***	37	24.5	***
		Control	78	20.5			29.5		
3		Rapamycin	73	25.7	28.5	***	34	13.5	***
		Control	76	20			29.5		
4		Metformin	100	24	20	***	34	23	***
		Control	67	20					
5		Allantoin	58	25.3	21.6	***	34.5	19.7	***
		Control	54	20.8			28.8		
6		Met + Rap	57	24.4	34	***	33	13	***
		Met	58	24	31.9	***	29.8	2	ns
		Rap	48	24	31.9	***	32	9.6	**
		Control	39	18.2			29.2		
7		Met + Rif	46	23.4	9	ns	31	9.5	***
		Rif	45	29.2	36	***	39.2	38.5	***
		Control	49	21.46			28.3		
8		Rap + Rif	44	32.2	49.7	***	41	44.9	***
		Rap	65	27.4	27.4	***	37	30.7	***
		Rif	45	29.2	35.8	***	39.2	38.5	***
		Control	49	21.5			28.3		
9		Rif + Psora	53	31.2	48.5	***	39.8	40.9	***
		Rif	60	27	28.6	***	37	30.9	***
		Psora	52	24.5	16.6	*	33.5	18.6	***
		Control	41	21			28.25		
10		Met + Psora	46	24.2	11.5	*	38.6	30.4	***
		Met	61	28.4	30.9	***	39	31.75	***
		Psora	52	24.5	12.9	*	33.5	13.2	*
		Control	53	21.7			29.6		
11		Met + Allan	34	24.25	16.6	ns	33.5	16.3	***
		Met	58	25.27	21.8	**	33.8	17.3	***
		Allan	41	25.36	22	**	34	18	***

		Control	54	20.8			28.8		
12		Rap+Allan	28	19.9	3	ns	30.3	-	ns
		Rap	31	24.3	26.23	**	33.6	-	ns
		Allan	47	23.6	22.6	**	30.8	-	ns
		Control	35	19.25			30.25	-	
13		Rap+Psora	60	23.5	10.8	ns	34.8	17.3	**
		Rap	62	24.35	14.9	*	32.8	10.5	**
		Psora	52	24.5	15.6	*	35.5	19.6	**
		Control	48	21.2			29.67		
14		Rif+Allan	46	26.5	38	***	35.8	26.5	***
		Rif	46	27.45	43	***	38.6	36.4	***
		Allan	56	23.6	22.9	**	34.16	20.7	***
		Control	44	19.2			28.3		
15		Psora+Allan	44	21.2	10.4	ns	33.5	18.37	***
		Psora	37	23	19.8	**	34	20.1	***
		Allan	56	23.6	22.9	**	34.16	20.7	***
		Control	44	19.2			28.3		
16		Rap+Rif+Allan	122	39.2	96.6	***	49.9	76.3	***
		Rif+Psora+Allan	138	37.7	89.5	***	49.85	76.15	***
		Rif+Psora	46	30	50.7	***	41.2	45.6	***
		Rap+Rif	39	28	40.7	***	40.5	43	***
		Rap	62	24.3	22	***	32.8	16	***
		Rif	60	27	35.7	***	37	30.7	***
		Psora	52	24.5	23	***	33.5	18.37	***
		Allan	56	23.6	18.6	***	34	20	***
		Control		19.9			28.3		
17		Rap+Rif+Met	31	20	-6.8	ns	32.3	14	***
		Rap+Rif	45	32	49	***	41.4	46.3	***
		Rif+Met	46	23.4	9	ns	31	9.5	**
		Rap	65	27.4	27.7	***	37	30.7	***
		Rif	45	29.24	36.25	***	39.2	38.5	***
		Control	50	21.46			28.3		
18		Rap+Rif+Psora	58	25.8	21.7	**	35	17.8	***
		Rap+Rif	64	27.46	29.8	***	38.4	29.3	***
		Rap	62	24.4	15	*	32.8	10.4	*
		Control	44	21.2			29.7		
19	daf-16	Rap+Rif+Allan	113	28	47.4	***	36.3	47.5	***
		Rif+Psora+Allan	128	26	36.8	***	33.8	37.4	***
		Rap+Rif	120	27.5	44.7	***	35.3	43.5	***
		Rif+Psora	130	28	47.4	***	34	38.2	***
		Rap	164	24	26.3	***	31	26	***
		Rif	113	19	0	ns	26.35	7	***
		Psora	197	20	5	*	27.2	10.5	***
		Allan	145	24	26.3	***	33.3	35.37	***
		Control	146	19			24.6		
20	daf-2	Rap+Rif+Allan	151	55.4	21	*	69.22	16	*
		Rif+Psora+Allan	132	46	0	ns	54.6	1.6	*
		Rap+Rif	125	55	20.4	*	69.6	16.7	*
		Rif+Psora	141	47.7	4.4	ns	57.7	-6.8	ns
		Rap	147	54.8	20	*	67.7	13.6	*
		Psora	134	58.5	28	*	71.4	19.8	*
		Control	78	45.7			59.6		

21	eat-2	Rap+Rif+Allan	36	33.2	33	*	44.25	39.15	*
		Rif+Psora+Allan	39	36.5	46	*	46	44.65	*
		Rap+Rif	43	33	32	*	43.4	36.5	*
		Rif+Psora	45	37.4	49.6	*	47.8	50.3	*
		Rap	35	26	4	ns	31.8	0	ns
		Rif	50	30.8	23.2	*	40	25.8	*
		Psora	37	27.9	11.6	ns	34.25	8	*
		Allan	37	25.5	2	ns	33.5	5.3	ns
		Control	42	25			31.8		
		Control N2	51	20			27.8		
22	daf-7	Rap+Rif+Allan	79	27.3	16.6	**	37.8	13.8	***
		Rif+Psora+Allan	89	27	15.4	**	36.5		***
		Rap+Rif	85	26.4	13	ns	37		***
		Rif+Psora	89	26.6	13.7	ns	37		***
		Rap	93	22.8	-2.5	ns	31		ns
		Rif	83	26.7	14	*	35.4		*
		Psora	85	23.6	-	ns	32.9		ns
		Allan	79	23.13	-	ns	31		ns
		Control daf-7	90	23.4			33.23		
		Control N2	68	18.8			28.6		
23	Flies	Rap+Rif+Allan	77	42	76.6	**	61.22	76.6	**
		Rap+Rif	83	38.8	63.2	**	57.22	65	**
		Rif+Psora+Allan	53	29	22	ns	46.5	34	**
		Rif+Psora	83	27.5	15.6	ns	50	43.5	**
		Rap	93	32.9	38.4	*	51.3	50	**
		Rif	92	26.3	10.6	ns	44.17	27.36	**
		Psora	83	27	13.5	ns	41	18.23	<0.01
		Control	90	23.8			34.67		
		Allan	80	37.2	15	*	50.12	-	ns
		Control	80	32.4			51.5		

*** = P value < 0.0001, ** = P value < 0.001, * = P value < 0.05

References

1. Chen, D., et al., *Germline signaling mediates the synergistically prolonged longevity produced by double mutations in daf-2 and rsks-1 in C. elegans.* Cell Rep, 2013. **5**(6): p. 1600-10.
2. Bjedov, I., et al., *Mechanisms of life span extension by rapamycin in the fruit fly Drosophila melanogaster.* Cell Metab, 2010. **11**(1): p. 35-46.
3. Robida-Stubbs, S., et al., *TOR signaling and rapamycin influence longevity by regulating SKN-1/Nrf and DAF-16/FoxO.* Cell Metab, 2012. **15**(5): p. 713-24.
4. Golegaonkar, S., et al., *Rifampicin reduces advanced glycation end products and activates DAF-16 to increase lifespan in Caenorhabditis elegans.* Aging Cell, 2015. **14**(3): p. 463-73.
5. De Haes, W., et al., *Metformin promotes lifespan through mitohormesis via the peroxiredoxin PRDX-2.* Proc Natl Acad Sci U S A, 2014. **111**(24): p. E2501-9.
6. Cabreiro, F., et al., *Metformin retards aging in C. elegans by altering microbial folate and methionine metabolism.* Cell, 2013. **153**(1): p. 228-39.
7. Onken, B. and M. Driscoll, *Metformin induces a dietary restriction-like state and the oxidative stress response to extend C. elegans Healthspan via AMPK, LKB1, and SKN-1.* PLoS One, 2010. **5**(1): p. e8758.
8. Ye, X., et al., *A pharmacological network for lifespan extension in Caenorhabditis elegans.* Aging Cell, 2014. **13**(2): p. 206-15.
9. Calvert, S., et al., *A network pharmacology approach reveals new candidate caloric restriction mimetics in C. elegans.* Aging Cell, 2016. **15**(2): p. 256-66.
10. Wan, Q.L., et al., *Aspirin extends the lifespan of Caenorhabditis elegans via AMPK and DAF-16/FOXO in dietary restriction pathway.* Exp Gerontol, 2013. **48**(5): p. 499-506.
11. Ayyadevara, S., et al., *Aspirin inhibits oxidant stress, reduces age-associated functional declines, and extends lifespan of Caenorhabditis elegans.* Antioxid Redox Signal, 2013. **18**(5): p. 481-90.
12. Petrascheck, M., X. Ye, and L.B. Buck, *An antidepressant that extends lifespan in adult Caenorhabditis elegans.* Nature, 2007. **450**(7169): p. 553-6.
13. Zarse, K. and M. Ristow, *Antidepressants of the serotonin-antagonist type increase body fat and decrease lifespan of adult Caenorhabditis elegans.* PLoS One, 2008. **3**(12): p. e4062.
14. Heidler, T., et al., *Caenorhabditis elegans lifespan extension caused by treatment with an orally active ROS-generator is dependent on DAF-16 and SIR-2.1.* Biogerontology, 2010. **11**(2): p. 183-95.
15. Tong, J.J., et al., *Life extension through neurofibromin mitochondrial regulation and antioxidant therapy for neurofibromatosis-1 in Drosophila melanogaster.* Nat Genet, 2007. **39**(4): p. 476-85.